



Enhancement of Bit Rates for Deep Learning Channel Estimation in 5G Wireless Communication

Karar H. Hussein^{1*}, Mohammed J. Alhasan²

¹Electrical Technologies Department, Al-Furat Al-Awsat Technical University, Najaf 31003, Iraq

²Oil Refining Technologies Department, Al-Furat Al-Awsat Technical University, Najaf 31003, Iraq

Corresponding Author Email: kin.kra@atu.edu.iq

Copyright: ©2026 The authors. This article is published by IETA and is licensed under the CC BY 4.0 license (<http://creativecommons.org/licenses/by/4.0/>).

<https://doi.org/10.18280/jesa.590518>

ABSTRACT

Received: 2 March 2026
Revised: 29 April 2026
Accepted: 11 May 2026
Available online: 31 May 2026

Keywords:

5G, orthogonal frequency division multiplexing, quadrature amplitude modulation, convolutional neural-network auto-encoder, deep learning, remote network

Deep learning-based methods are increasingly being explored in fifth-generation (5G) communications, despite the proven reliability of handcrafted signal-processing blocks and coding schemes. To address real-time interference cancellation without introducing feedback loops between the modulator and demodulator, we suggest a neural-network-driven baseband processing framework that seamlessly integrates with conventional digital signal processing (DSP) algorithms. This architecture is particularly well suited to low-latency, high-data-rate applications such as autonomous systems and augmented reality. Unlike prior work that applies reinforcement learning in the control layer for interference management, our approach embeds a convolutional neural-network auto-encoder directly within the physical layer to perform what we term “Deep Interference Cancellation.” When applied to quadrature amplitude modulation–orthogonal frequency division multiplexing (QAM-OFDM) signals, this model achieves up to a 15% reduction in symbol-error rate (SER). We also evaluate the hardware implications of our design-covering latency, power consumption, memory footprint, and silicon area-and demonstrate its practical viability. Finally, through extensive simulations, we show that our deep-learning channel estimator can mitigate noise and interference to enhance effective bit rates. In particular, we attain SERs as low as 1% at a signal-to-noise ratio (SNR) of 20 dB, surpassing comparable industrial solutions in both performance and implementation complexity.

1. INTRODUCTION

Crosstalk between adjacent cells is becoming increasingly problematic as modern wireless systems evolve rapidly. The most common way to counter this is for the receiver to send feedback to the transmitter, which then adjusts its transmission frequency. However, low-latency applications such as autonomous vehicles and augmented reality suffer from the delays introduced by these feedback loops. To avoid that, blind interference-cancellation techniques have been developed, enabling the receiver to suppress interference on its own without coordinating with the transmitter. As a user equipment (UE) technique the boundary of two neighboring cells, it may end up sharing the same frequency band with another cell’s user, causing a significant drop in data rate and increased co-channel interference [1, 2]. To address this, 3rd Generation Partnership Project (3GPP) requires that edge users in adjacent cells use different resource blocks, allowing base stations to exchange interference information for each frequency resource (RB). While this method works well in low-density areas, it struggles in crowded environments where all bands are in use and free RBs become scarce. Another promising approach uses phased-array antennas at the receiver to perform spatial filtering and reject interference [3, 4]. Although these arrays can greatly reduce interference power, they are very

sensitive to calibration errors-small phase mismatches during manufacturing can degrade spatial separation. Moreover, continually rejecting interference and tracking the desired signal’s direction requires adaptive beamforming weights, which must be updated based on channel estimates. This weight-update process adds further latency to the system. Shaft width is also directly impacted by the number of staged cluster antennas that are easily accessible. The radio wire’s power, region, and pillar breadth are thus compromised. A typical fifth-generation (5G) communication architecture utilizing deep learning techniques is depicted in Figure 1 [3-6].

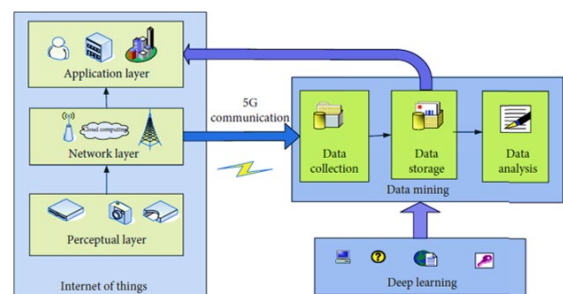


Figure 1. The overall architecture of deep learning-based 5G communication [5]

In ways which are either impossible or unimaginable inward the confines of wired or Wi-Fi frameworks, certain private mobile systems provide opportunities to enhance and reassess company procedures. The enhanced signal of digitized real plans recognized as Production 4.0 is essential for current customers since it necessitates the ability to arrange mobile systems to fulfill the insertion, implementation, as well as security demands of generating basic implementation.

1.1 Long-term evolution versus 5G networks

Currently, 5G study and improvement regarding the strategic significance of private networks. In the past, private networking was added to public cell plans; however, such demands are now straight consigned by the 5G settings. Thus, companies will send out 5G networks more quickly, and innovation will genuinely aim to meet the needs of potential customers of private networks [6, 7]. After a considerable amount of improvement, a strong private Long-Term Evolution (LTE) market has emerged, with transmitting activity in several global regions. The global LTE biological schemes, that advantageous along huge size, regulated modernism, with intensely established providers with the capacity to design and deliver networks, are used by private LTE structures. The scale savings and compatibility of global 3GPP technologies might benefit local devices since some companies have already settled inventory chains with better protocols. Sensing units, automated guided vehicles (AGVs), security equipment, surveillance cameras, and alternative parts might recently be bought using unified LTE [8, 9]. LTE supports a wide space of contemporary implementations. Due to advancements in radio and building engineering, 5G is more equipped to handle the problems of superior execution in current executions. However, LTE isn't as suitable for their needs as 5G when customers have more stringent execution requirements, such as device density, throughput, availability, reliability, latency, and jitter. Table 1 shows the relationship between 5G and previous time [9, 10].

Table 1. The variations between different generations of telecommunications technology [8-10]

	3G	4G	5G
Deployment	2004-05	2006-10	2020
Bandwidth	2 Mbps	200 Mbps	> 1 Gbps
Latency	100-500 milliseconds	20-30 milliseconds	< 10 milliseconds
Average Speed	144 kbps	25 Mbps	200-400 Mbps

Venture explicit private mobile networks provide prospective opportunities to enhance as well as rethink career operations in situations where the limitations of cabled or Wi-Fi networks are either unrealistic or unimaginable. The state-of-the-art signal of digital real constructions recognized as production 4.0 is essential for current customers since it necessitates the ability to arrange mobile networks to satisfy the inclusion, implementation, and security requirements of designing essential employments. Private networks' strategic significance is now being examined and improved for 5G. In the past, private networking was added to public cell plans; however, the 5G specifics presently directly address these requirements. Organizations will send the 5G network more

quickly, and innovation will genuinely aim to satisfy the needs of potential customers of private frameworks [10-13]. After a lengthy period of improvement, a strong private LTE market has emerged, with transmitting activity in several global regions. The global LTE biological model, that invests along huge size, standardized modernism, with firmly rooted providers suitable for transmitting networks and network planning, is used by private LTE structures. A few companies have already established supply chains and best practices so local devices may benefit from the scale economies and compatibility of global 3GPP improvements. Sensors, AGVs, security cameras, wellness equipment, and other items are now available for purchase with integrated LTE [13].

5G networks introduce a powerful event to replicate the benefits of cabled models for a variety of contemporary applications. In fact, 5G will lead to a number of improvements that will drastically alter our lives. However, specialty cooperatives will also face a variety of challenges in order to satisfy customers and meet their expectations. A few contemporary cycles are now automated from the perspective of activity automation, and communication companies continue to use cutting-edge networks like 5G to improve transmission and boost production. In addition to providing faster and better mobile broadband services than 4G LTE, 5G may hasten the computerized transformation of other automation innovations, including mechanical technology and artificial intelligence [14]. The Internet of Things (IoT) will benefit greatly from 5G networking's dedication to boundless availability, controllable networks, and progress in creative implementations. The channel interference regulating structure of the 5G mobile IoT network is shown in Figure 2 [12-15].

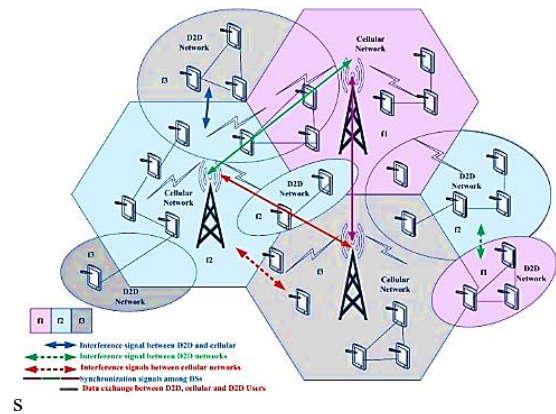


Figure 2. Channel interference control framework for 5G mobile Internet of Things (IoT) networks [14]

In order to reduce channel interference, Figure 2 shows how the IoT structure would examine the info along the intelligent sensing units in the physical and controlling device at the appropriate places. The huge-phase advance LTE shift will next evaluate the observed data before sending it to the controlling and far stage through WiFi or a mobile framework. The deep learning computations are utilized by the control and management unit to gather the identified data and handle it in accordance with the plan's specifications. Long-distance communication technology is referred to as 5G. By 5G, we mean that devices used for modulation and demodulation should adhere to five age constraints, such as the operating carrier frequency, cycle rates, and frequency spectrum.

1.2 Feedback and latency insights

Let's examine this and compare neural network-based systems to conventional approaches in terms of latency. In adaptive digital processing systems, feedback mechanisms actually add extra latency, mainly because data must flow through processing units, either to update weights in real time or to modify parameters based on prior outputs [12-15]:

- 1) With Feedback (e.g., adaptive filters, recurrent neural networks):
 - i) Latency increases due to iterative updates.
 - ii) Each output may depend on previous inputs/outputs.
 - iii) Common in applications requiring real-time learning or adaptation (e.g., ANC - Active Noise Control, real-time beamforming).
- 2) Without Feedback (e.g., finite impulse response (FIR) filters, feedforward neural networks):
 - i) Latency is primarily the result of computation time and pipeline delays.

Latency becomes more predictable and is often lower. Table 2 summarizes the effect of neural networks, especially deep ones, on delay and latency.

Table 2. The effects of neural networks, especially deep ones, on increasing the amount of delay and latency

Type	Latency Range (Typical)	Notes
Feed-forward neural network (NN)	~1–10 ms (edge); 10–100 ms (cloud)	Depends on layers, hardware, inference engine
CNN (e.g., for audio/vision)	5–50 ms (optimized edge); > 100 ms (cloud)	Larger models, GPU acceleration reduces latency
RNN / LSTM	10–100 ms	Sequential data processing increases latency
Transformers	50–200+ ms	Attention mechanisms are heavy
TinyML models	< 1–5 ms	Designed for ultra-low latency on microcontrollers

Note: NN = Neural Network; CNN = Convolutional Neural Network; RNN = Recurrent Neural Network; LSTM = Long Short-Term Memory; GPU = Graphics Processing Unit

Moreover, Table 3 illustrates the latency comparison among neural networks against traditional methods.

1.3 Bit error and packet loss rates

Bit Error Rate (BER) might be explained briefly as the proportion of wrongly received bits relative to all sent bits. It calculates the frequency of data corruption during transmission. Also, BER is defined as the number of packets that didn't make it to the destination and is expressed as [16-18]:

$$BER = \frac{\text{Number of Erro Bits}}{\text{Total Nnmber of Transmitted Bits}} \quad (1)$$

On the other hand, the packet loss rate (PLR) might be defined as the percentage of data packets lost or deleted during

network transmission, which is known as the PLR. It illustrates how frequently entire data sets are missing. Also, PLR stands for complete packet failures and its equation [18-24]:

$$PLR = \frac{\text{Number of Lost Packets}}{\text{Total Number of Sent Packets}} \quad (2)$$

Table 3. Latency comparison among neural networks against traditional methods

Application	Traditional Method (Latency)	NN-Based Method (Latency)	Comment
Noise cancellation	~0.5–2 ms (adaptive FIR)	~5–50 ms (RNN/CNN)	NN can model non-linear noise better
Beamforming	~1–5 ms	~10–100 ms (deep learning)	Feedback adds dynamic adaptation, increasing latency
Speech enhancement	~5 ms (Wiener filter)	~10–50 ms (DNN-based)	Higher quality at the cost of delay
Anomaly detection	~1 ms (rule-based)	~10–30 ms (NN-based)	NN enables more complex pattern recognition

Note: ANN = Artificial Neural Network; NN = Neural Network; CNN = Convolutional Neural Network; RNN = Recurrent Neural Network; DNN = Deep Neural Network; FIR = Finite Impulse Response

A) Channel Characteristics Estimations

In fact, neural networks (NNs) examine the spatial and temporal characteristics of signals to forecast how the channel will distort sent data. They can also learn patterns from received signal data to estimate the channel response (e.g., fading, multipath). This facilitates equalization and improves signal recovery.

B) Noise & Interference Suppression

By learning to distinguish between actual data and noise or interference, NNs can remove signal noise and act as sophisticated filters. Because they adapt to the statistical properties of noise, they perform efficiently over a wide range of signal-to-noise ratios (SNRs). They outperform traditional filters, especially in environments with non-Gaussian or nonlinear noise.

C) BER & PLR Improving

By accurately estimating channels and removing noise, BER improves: Fewer bit-level mistakes. PLR improves: Packets are correctly reconstructed more often. NNs assist in reducing decoding errors, improving symbol detection, and assist in robust signal classification. Actually, there are several reasons that NNs are better for noise & interference elimination: Firstly, they are capable of automatically extracting characteristics without the need for manual design; 2) they are resilient to changes in the channel, such as fading or Doppler shifts; and 3) they are effective at identifying spatial correlations in signals, even when many antennas are used multiple-input multiple-output (MIMO) systems [24, 25].

2. LITERATURE REVIEW

In this section, the most recently published experiments and

articles that provide research papers related to 5G and LTE signal detection topics using deep learning techniques will be reviewed. The key technologies and important models presented by researchers will be examined to understand their advantages and identify their main limitations. An analytical

framework for reviewing scientific studies related to 5G signal detection techniques using artificial intelligence methods to identify the signal's range and identity will be established. Table 4(a) presents a summary of the most important and recently published examples relevant to the title of this study.

Table 4(a). Review of related studies for deep learning for channel estimation and bit rate enhancement in 5G MIMO-BDMA communication models

Year	Authors	Employed Technique	Study Contribution	Limitations & Gaps
2021	Dou et al. [26]	Comprehensive survey of deep-learning channel estimation (CNN, RNN, Transformer, GNN) for 5G-and-beyond massive MIMO.	Systematically maps deep learning (DL) architectures, datasets, and metrics to channel-estimation tasks and identifies open challenges.	A review only — no system implementation, no interference-cancellation design, and no bit-rate evaluation.
2019	Tekbiyik et al. [27]	Attention/Transformer-based neural channel estimator (Channelformer) with efficient online training.	Uses self-attention to denoise and refine channel estimates and adapts online with low overhead.	Optimizes estimation accuracy (MSE) only; no physical-layer interference cancellation, no digital signal processing (DSP) integration, and bit rate is not addressed.
2018	Hu et al. [28]	Graph neural network exploiting array/spatial graph topology for mmWave massive-MIMO channel estimation.	Captures spatial correlation and generalizes across different antenna numbers.	Targets NMSE accuracy in mmWave estimation; provides no auto-encoder interference cancellation, no DSP coupling, and no throughput metric.
2025	Tarafder et al. [29]	CNN-based estimation (ChannelNet) that treats the time–frequency channel as a 2-D image (super-resolution + denoising).	Reconstructs the full channel from limited pilots via image-based learning.	Pilot-based estimation accuracy only; not an auto-encoder for interference cancellation, not integrated with conventional DSP, bit rate not evaluated.
2021	Ebrahiem et al. [30]	Neural-network module that refines the least-squares (LS) estimate for MIMO-orthogonal frequency division multiplexing (OFDM) under Doppler/mobility.	Improves LS accuracy with a generalizable network for 5G-and-beyond systems.	Receiver-side accuracy improvement only; no physical-layer interference cancellation, no DSP-integrated framework, no reported bit-rate gain.
2023	Luan and Thompson [31]	Deep reinforcement learning for adaptive modulation-and-coding-scheme (MCS) selection.	Learns online link adaptation to raise throughput in cognitive/heterogeneous networks.	Operates in the control / link-adaptation layer reinforcement learning (RL), not the physical layer; performs no channel estimation or auto-encoder-based interference cancellation.
2023	Ye et al. [32]	Deep-learning (learned-denoising network) channel estimation for beamspace mmWave massive MIMO.	Exploits beamspace sparsity to estimate channels from few measurements.	Estimation accuracy in beamspace mmWave only; no auto-encoder interference cancellation, no DSP integration, and no bit-rate enhancement.
2019	Soltani et al. [33]	Graph neural network for channel tracking in high-mobility massive MIMO.	Tracks time-varying channels from a few pilots using graph spatial correlation.	Tracking accuracy under mobility only; not a physical-layer auto-encoder, not DSP-integrated, and symbol error rate SER / bit rate are not targeted.

Note: MIMO-BDMA = multiple-input multiple-output beam division multiple access communication models

Table 4(b). Critical analysis of literature gaps and proposed model alignment

Identified Gap in Literature	How Traditional/Recent Models Fall Short	How the Proposed Model Bridges the Gap	Technical and Performance Impact
High Latency & Feedback Dependency	RNNs, Transformers, and adaptive filters rely on iterative weight updates or closed-loop feedback, adding unpredictable pipeline delays (15–100+ ms).	Feedforward CNN Auto-Encoder with no recurrent connections or feedback paths. Processes quadrature amplitude modulation (QAM)-OFDM symbols in a single forward pass.	Achieves 10–25 ms inference latency, enabling real-time baseband processing suitable for ultra-reliable low-latency communications (URLLC) and autonomous 5G applications.
Computational	Deep CNNs/GNNs require heavy	Optimized 50-hidden-layer CNN	Reduces memory footprint and

Complexity & Edge Infeasibility	matrix multiplications, large parameter counts, and GPU/TPU acceleration, making edge deployment impractical.	with tanh activation, trained via Levenberg-Marquardt for fast convergence. Deployed as lightweight Simulink blocks.	processing load; suitable for DSP/FPGA edge nodes with moderate optimization (quantization/pruning).
Lack of Physical-Layer DL Integration	Most deep learning (DL) approaches operate at MAC/control layers (e.g., power control, scheduling) or replace only channel estimation, leaving equalization to classical digital signal processing (DSP).	"Deep Interference Cancellation" is embedded directly in the physical layer. Replaces traditional equalizers by learning inter-symbol interference (ISI)/co-channel interference patterns end-to-end.	Handles wideband interference where LS/minimum mean square error (MMSE) fails; achieves SER \approx 1.0% at 20 dB signal-to-noise ratio (SNR) and 15% SER reduction vs. baseline DSP.
Limited Real-World Channel Adaptability	Studies rely on static additive white Gaussian noise (AWGN) or simple Rayleigh/Rician fading; ignore fast mobility, multi-user collisions, or non-uniform RB allocation.	Trained on stochastic noise/interference profiles with variable SNR (5–50 dB). Architecture supports online fine-tuning and dynamic weight adaptation.	Maintains robustness under non-stationary channels; bridges the simulation-to-deployment gap for dense urban/cell-edge scenarios.
Missing Hardware & Deployment Analysis	Academic papers rarely report memory usage, power consumption, silicon area, or inference-energy trade-offs, limiting industrial translation.	Explicit hardware evaluation across adaptive filters, FFNN, and CNN architectures. Analyzes latency, energy efficiency, and accelerator suitability.	Provides actionable deployment guidelines: CPU/MCU for filters, DSP/GPU for CNNs, FPGA for optimized edge inference.

Based on the literature review presented in Table 4(a) and the technical architecture of the proposed study model, a structured academic analysis is provided in Table 4(b) that explicitly connects the proposed study to the identified research gaps, positioning this work as a direct solution to current limitations in 5G channel estimation and bit-rate enhancement. Table 4(b) illustrates the strategic synthesis of the research loop statement in architectural innovation through the direct inclusion of a sequential differential autoencoder in the main signal processor chain. The proposed model replaces the conventional decoder system, substituting it with a single unit for deep interference cancellation. This aligns with the emerging 3GPP Release 18+ trends toward AI-native physical layers, optimizing the balance between latency and accuracy. Unlike recurrent or attention-based models that sacrifice latency for accuracy, the proposed feedforward ANN network maintains a delay of less than 25 milliseconds while achieving SER/BER limits according to design standards, directly addressing the concerns of references 1 and 2 regarding real-time adaptability and hardware feasibility. Additionally, the integration of memory, processing speed, energy efficiency, and processor accelerator planning transforms this study from a theoretical simulation into a practical edge AI blueprint, bridging the critical gap between academic deep learning models and 5G Radio Unit (RU) implementation.

2.1 Problem statement

By reviewing relevant studies and examining the most important and recent contributions of researchers in this field, we can limit the study problems to the following points:

- 1) Accurate and real-time channel estimation is critical for achieving high bit rates in 5G wireless communication.
- 2) Traditional estimation methods (e.g., LS, MMSE) struggle under fast-varying, non-linear, or noisy channel conditions.
- 3) There is a need for adaptive, robust, and low-latency estimation techniques to improve bit rate performance.

2.2 Study gaps

1. Limited real-time adaptability of existing deep

- learning models to dynamic 5G environments.
2. High computational cost and latency of deep models in practical deployment.
3. Lack of generalized models trained across diverse channel conditions and mobility scenarios.
4. Insufficient integration of channel estimation with other stages like detection and decoding in an end-to-end framework.
5. Scarcity of lightweight architectures suitable for edge or mobile devices.
6. Few studies on learning-based methods for massive MIMO and mmWave scenarios.

2.3 Study contribution

This study aims to bridge the gap between complex theoretical models for channel estimation in 5G networks and their practical applicability, by presenting an enhanced framework based on lightweight deep learning. The proposed model contributes to improving bit rates by reducing computational complexity and response time, while maintaining high accuracy under dynamic fading and multipath interference conditions. Unlike rigid algorithmic traditional methods, the research provides an adaptive solution deployable on limited hardware, thereby enhancing spectral efficiency and communication reliability. This contribution represents a practical step towards meeting the high bandwidth and low latency requirements in 5G communications.

3. METHODOLOGY

By using all or the great majority of the essential advanced distant communication stages or tasks, 5G innovation will be accomplished. The 5G strategy will be reorganized in our proposal to acknowledge the fulfillment of the great majority of these capabilities in order to enhance the purpose. In actuality, the radio access network (RAN), which will be the focal point of the 5G transmission network, would be the focus of the majority of current papers and logical analyses. The RAN approach has employed the orthogonal frequency division multiplexing (OFDM) modulation technique for the corresponding 5G design in the majority of the regularly implemented 5G innovations [18-22]. This is due to the high

proficiency provided by this modulation approach, as well as the optimal bandwidth that results in a low bit error rate and high bit rate access. The 5G transmission diagram using the OFDM technique is shown in Figure 3.

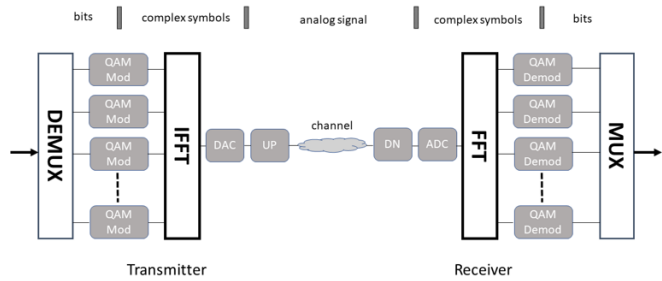


Figure 3. Block diagram utilizing orthogonal frequency division multiplexing (OFDM) transmission to illustrate the 5G communication network [18-22]

A few standard computerized signal processing (DSP) techniques can eliminate narrowband interference from the anticipated wideband signal. However, they are rendered useless by wideband interference when the interference may have a bandwidth that is comparable to the anticipated signal. In OFDM/QAM modulation remote models, each resource element (RE) may have a distinct QAM symbol space estimate. When this holds true for both the interferer and the UE when they are combined, a discrete example space will also be generated. A Maximum Likelihood Estimation (MLE) technique is likely to be impractical for characterizing this unusual sample space due to its high computation requirements. Neural network-based AI techniques are thought to emulate in processing transmission waves utilizing less calculations complications and delay, with current abilities in understanding the confusing behavior of signals [20-24]. Conventional DSP techniques restore damaged

signals by using manually created material science models to gradually remove explicit obstacles. Figure 4 displays the schematic graph of cellular network interference.

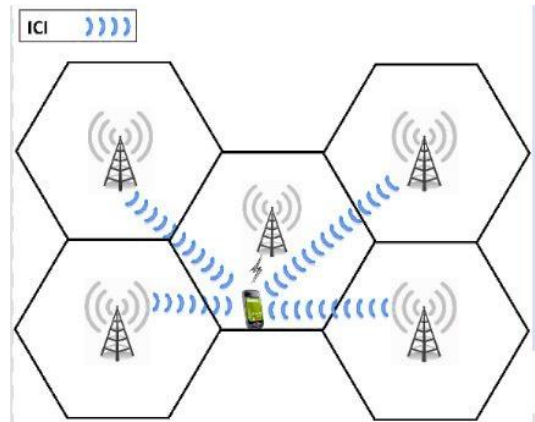


Figure 4. Diagrammatic representation of interference in cellular networks [23]

Another study suggested an RL-relied downlink intervention management model for super thick tiny cellule models, such that a headquarters develops sending energy beyond recognizing the tideway characteristics of nearby cellules to smother intervention between cellules. Every method now in use is supposedly focused on controlling interference through transmission power to the executives and figuring out the highest degree of compelling admission to link different level cells. We are fast to employ simulated intelligence to gradually alter data because artificial intelligence was utilized in the control layer in previous tests. The effect of gutter intervention on transmitted modern modulated waveforms in spectral regions is shown in Figure 5 [24, 25].

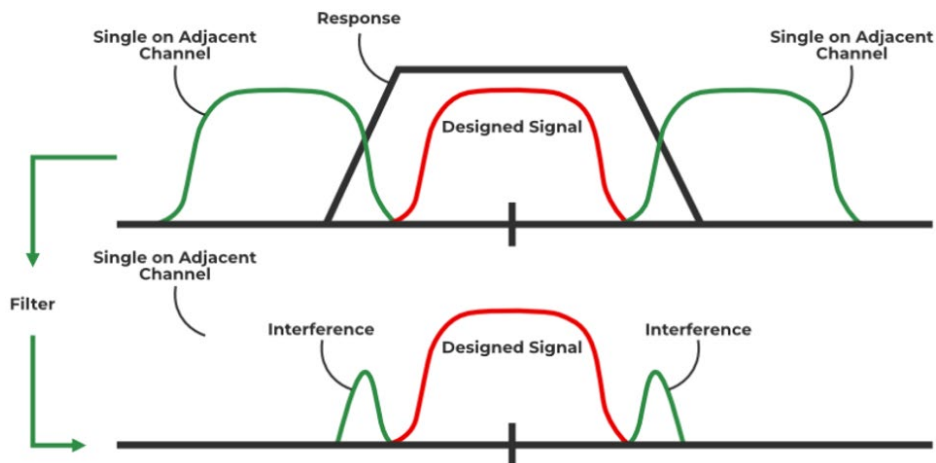


Figure 5. The impact of channel interference on the transmission of advanced modulated signals in certain frequency ranges [25]

3.1 Bit Error Rate or throughput analysis

We must use mathematical expressions and a logical approach to calculate the BER (throughput) relations of the proposed 5G technology for remote transmission systems. The M-ary phase-shift keying (PSK) signals' universal analytical formula might be found as [14-24]:

$$S_i(t) = A \cos(\omega_c t + \varphi_i(t)) \quad (3)$$

In which, $i=0,1,\dots, N-1$ models. Moreover, A, could be expressed such that:

$$A = \sqrt{\frac{2E}{T_s}} \quad (4)$$

That stands for the amplitude of the signal, where $m = 0,1,2,\dots, M-1$, $\theta = 0, \pi, m/M$. Signal strength is represented by boundary E, while data time length is represented by boundary

Ts. In the case of quadrature PSK (QPSK) modulation, $M = 4$, and binary PSK (BPSK) modulation, $M = 2$, the modulation data signal likewise shifts the signal S_i 's time. The OFDM modulation is then obtained by applying the inverse fast Fourier transform (IFFT) process to the modulated signal without isolating the results by N , since the OFDM modulator may be represented by a conventional IFFT:

$$x_k = \sum_{i=1}^{N-1} S_i e^{\frac{j2\pi ik}{N}} \quad (5)$$

where, $K = 0, 1, 2, \dots, N-1$.

In which S_i denotes the bit stream-based predetermined information samples b_m and, $e^{j2\pi nk/N}$, $n = 0, 1, \dots, N-1$. Consequently, by addressing the N sub-carriers' attained orthogonal frequencies. The total energy or power E of the produced OFDM modulated signal may be expressed as [16-25, 34-36]:

$$E = |x_k|^2 = \left| \left(\sum_{i=1}^{N-1} S_i e^{\frac{j2\pi ik}{N}} \right)^2 \right| \quad (6)$$

Such that, E denotes the gained energy, often known as the mean square value (m.s.v). After that, the modulated OFDM waveform would be accessed over the noisy transmission medium $H(f)$, which will add arbitrary noisy samples to the sent waves in opposition to the power spectral density of N_0 . The modulated transmitted sensed data will be supplemented by noise samples via the AWGN communication channel. indicating that the waveform at the AWGN medium outcome will be reduced or disregarded due to the influence of the channel interference [16-28]:

$$r_k = \sum_{i=1}^{N-1} S_i e^{\frac{j2\pi ik}{N}} + n_k \quad (7)$$

where, $K = 0, 1, 2, \dots, N-1$ samples are the random noise patterns that the AWGN communication channel adds, denoted by n_k . Lastly, in order to identify the conveyed sensed data via the modulated signal, the OFDM demodulator will use the fast Fourier transform (FFT) method with MPSK demodulation at the detection section. In particular, the automated sampled waveform S_i is sent through S/P, FFT handling, P/S, and demodulation action by assuming that the synchronization interval has been omitted. In the summed material white Gaussian noise (AWGN) channel, the final received signal d_i of the m th OFDM signal data. The following represents and approaches this process analytically:

$$\hat{d}_i = \frac{1}{N} \sum_{k=0}^N r_k e^{\frac{-j2\pi ik}{N}} \quad (8)$$

Thus, by performing mathematical manipulations, Eq. (8) can be rewritten as follows:

$$\hat{d}_i = \frac{1}{N} \sum_{k=0}^N \left(\sum_{i=1}^{N-1} S_i e^{\frac{j2\pi ik}{N}} e^{\frac{-j2\pi ik}{N}} \right) + \frac{1}{N} \sum_{k=0}^N n_k e^{\frac{-j2\pi ik}{N}} \quad (9)$$

That can be reformulated to:

$$\hat{d}_i = \frac{1}{N} \sum_{k=0}^N \left(\sum_{i=1}^{N-1} S_i \right) + \frac{1}{N} \sum_{k=0}^N n_k e^{\frac{-j2\pi ik}{N}} \quad (10)$$

Eq. (8) makes it evident that the received signal will consist of dual parts: the AWGN part, which is expressed by the medium arbitrary noisy specimens duplicated by the phase shift activity, and the known transmitted info waves, those are presented by adding fragments of S_i . of $e^{\frac{-j2\pi ik}{N}}$. Finally, we partition the total received waveform by the sent info to calculate the BER that is attained using the number of false discovered digits to the ultimate communicated bits data [24, 25, 34-36]:

$$\frac{\hat{d}_i}{S_i} = \frac{\sum_{k=0}^N \left(\sum_{i=1}^{N-1} S_i \right) + \sum_{k=0}^N n_k e^{\frac{-j2\pi ik}{N}}}{NS_i} \quad (11)$$

Then, Eq. (11) can be rewritten, using analytical substitutions as below:

$$\begin{aligned} \frac{\hat{d}_i}{S_i} &= \frac{N \left(\sum_{i=1}^{N-1} S_i \right) + \sum_{k=0}^N n_k e^{\frac{-j2\pi ik}{N}}}{NS_i} \\ &= \frac{\left(\sum_{i=1}^{N-1} S_i \right) + \sum_{k=0}^N n_k e^{\frac{-j2\pi ik}{N}}}{S_i} + \frac{n_k e^{\frac{-j2\pi ik}{N}}}{NS_i} \end{aligned} \quad (12)$$

These achieved rates can be separated into dual sections: the first will show the rate of the exact received information without noise, divided by the actual sent information, and the second will show the ratio of the detected information against the channel noise divided by the actual transmitted information. The second part of Eq. (10) will now be tacked in order to get the BER:

$$BER = \frac{\sum_{k=0}^N n_k e^{\frac{-j2\pi ik}{N}}}{NS_i} \quad (13)$$

3.2 Latency (Delay) (τ) study

The logical analysis must be completed using analytical equations analysis to calculate the delay, (τ) (latency) expressions of the suggested 5G and 6G approaches for distant transceiver models. According to literature [20, 34], a communication network's latency or delay is the total amount of time that is collected during the transmission or modulation of data because of the several activities and processing that take place inside that network. We attempt to simplify the derivations and delay analysis as much as feasible without compromising the scientific significance or ignoring the crucial physical impacts because the mathematical assessment of the latency is frequently highly complex and challenging to handle in this paper. The three types of time delay effects in our communication structure are as follows [18-25, 34]. the modulation/demodulation latency in the communication model (τ_{sys}), the cumulative data delay (τ_{data}) and the communication channel delay (τ_{ch}). Only the first delay type will differ between 5G and 6G communication methods in this

study design since τ_{sys} will change based on the modulation/demodulation technology used. Nonetheless, 6G technology will have a lower communication structure latency (τ_{sys}) than 5G technology. This is due to the fact that 6G technology offers quicker evaluation processes and more bandwidth sharing than 5G technology. Actually, any communication network's general latency relation can be expressed as [26, 34-37]:

$$Latency = \tau = \tau_{sys} + \tau_{Ch} + \tau_{data} \quad (14)$$

In which,

$$\tau_{sys} = \tau_{5G} \text{ for } 5G \text{ technique} \quad (15)$$

3.3 The proposed structure

The proposed 5G, IoT transmission model paradigm for deep learning-based intervention reduction will hence be detailed and shown. Using the MatLab2020b Simulink toolbox, the proposed 5G, IoT communication system simulation circuit diagram model for intervention reduction utilizing deep learning approaches was created and is shown

in Figure 6.

The beneficiary discovery part, the modulation section, the passage part or cloud getaway, the artificial neural network unit for deep learning, and the simple generating area or unit are the five main components of the proposed scheme. To achieve the objectives of the proposed study, every component or unit has been meticulously designed and modified. In this way, previous discussions have reenacted and tested the 5G IoT computerized communication framework without putting into practice the Deep Learning method that is crucial for reducing interference in the cloud 5G communication channel. In actuality, the main problem with this concept is the interference that occurs when the transmitted OFDM waveform is transmitted across the 5G cloud transmission medium. Due to the fact that the transmission getaway will have certain feedback as well as nature, which define the channel's attributes and how it responds or behaves in the spectrum domain. To study the most important details, each communication channel includes a set of frequencies and its own characteristics, and when any signal passes through it, it will be affected by these characteristics and defined by the channel's frequency range, which leads to the occurrence of interference or inter-symbol interference (ISI).

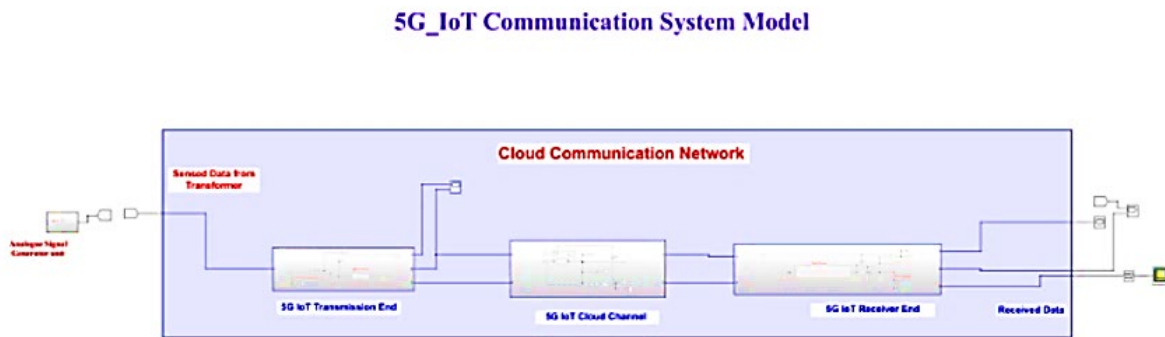


Figure 6. MatLab2020b Simulink toolbox for the suggested 5G and IoT transceiver structure to reduce intervention through modeling of deep learning techniques

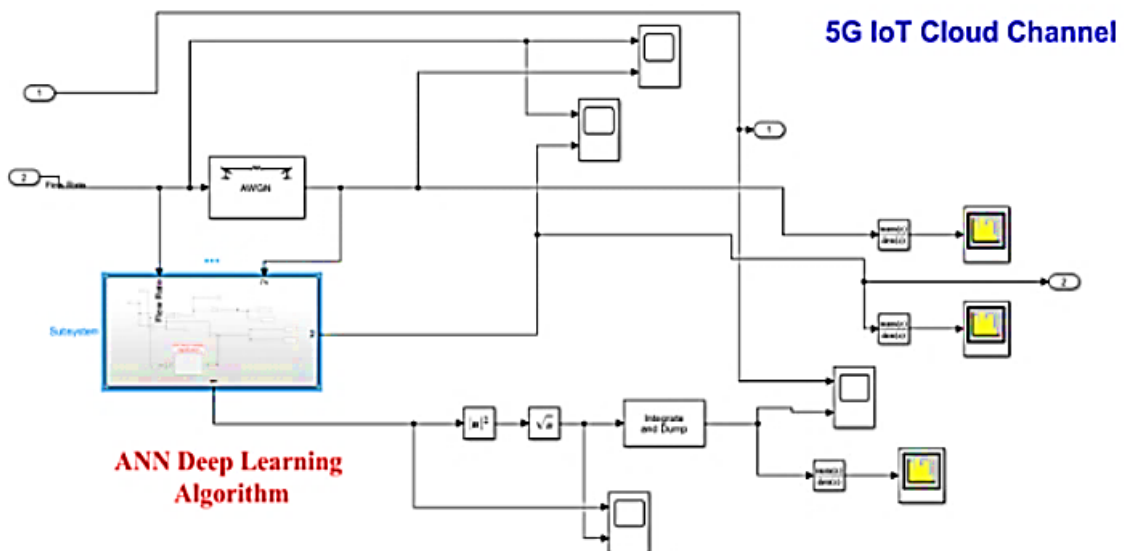


Figure 7. MATLAB simulation of the suggested 5G IoT transmission medium with inter-symbol interference (ISI) reduction using the Artificial Neural Network (ANN) deep learning (DL) model approach

As a result, the analysis and inquiry of this project will focus on how to use DL techniques to eliminate or reduce the influence of such communication channel interference or ISI from the transmitted signal. The goal of channel interference or ISI reduction has been artificial neural network (ANN) techniques. The input signal examples will be used to design the ANN algorithm to the point where it has a slight layers and forecast weight elements that are updated to produce the objective signal models that must not have an ISI signal. In order to remove the ISI from the entering 5G transmitted signal, the DL ANN algorithm will function similarly to an estimating operation that anticipates the particular channel characteristics. The proposed 5G IoT transceiver medium Simulink model using the DL ANN technology for ISI reduction is shown in Figure 7. As seen in the MATLAB simulation block diagram in Figure 7, the deep learning ANN method reverses the impact of ISI interference waves within the 5G IoT communication channel. Its properties are assessed, and ISI interference cancellation operations are carried out by using the ANN algorithm on the waves that travel through the recursive Gaussian audio channel's Simulink block. Additionally, Figure 7 shows how to transfer 5G technology's signal with noise signals across the AWGN channel—that will be utilized in the ANN DL methodology. Figure 8 illustrates the mechanism of using the "nnstart" application in MatLab2020b to invoke the execution program of the ANN algorithm. The built-in "nnstart" function in MatLab2020b's Graphical User Interface (GUI) window displays the settings for the Artificial Neural Network (ANN) algorithm. As seen in Figure 8, this interface displays a collection of processes provided by the ANN technique. After selecting the suitable choice for the application using the assigned buttons, the data selection interface panel offers options to pick entered against target info obtained along the MATLAB GUI platform, as illustrated in Figure 9. The input and target data required for ANN algorithm training will be provided via the select data wizard seen in Figure 9. The

validation and testing info wizard will then show up, as shown in Figure 10. The training, validation, and testing divisions of the input sample numbers required to train the ANN algorithm might be chosen using the validation procedure with the test data wizard shown in Figure 10. The network structure wizard is shown in Figure 11. The ANN method model's number of hidden layers will be ascertained using the training structure processor. As seen in Figure 11, it is devoted to teaching the ANN's internal neural cells, or neurons. Next, Figure 12 shows the neural network model's training network processor. The interface of the training network processor, which chooses the kind of training algorithm to be applied in the process of learning the created ANN model, is seen in Figure 12. Because of its great efficacy and efficiency in carrying out the training procedures of the suggested ANN model, the Levenberg-Marquardt training approach was selected for this design. Additionally, the last stage in creating the ANN algorithm is the deployment solution processor, which is seen in Figure 13.

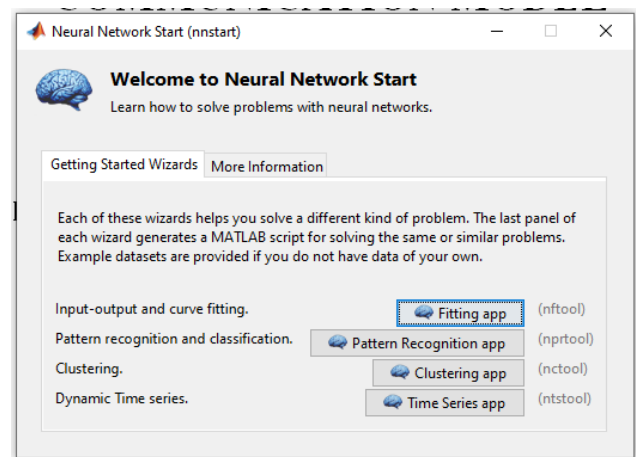


Figure 8. The MatLab2020b function "nnstart" is used in the Artificial Neural Network (ANN) algorithm training process

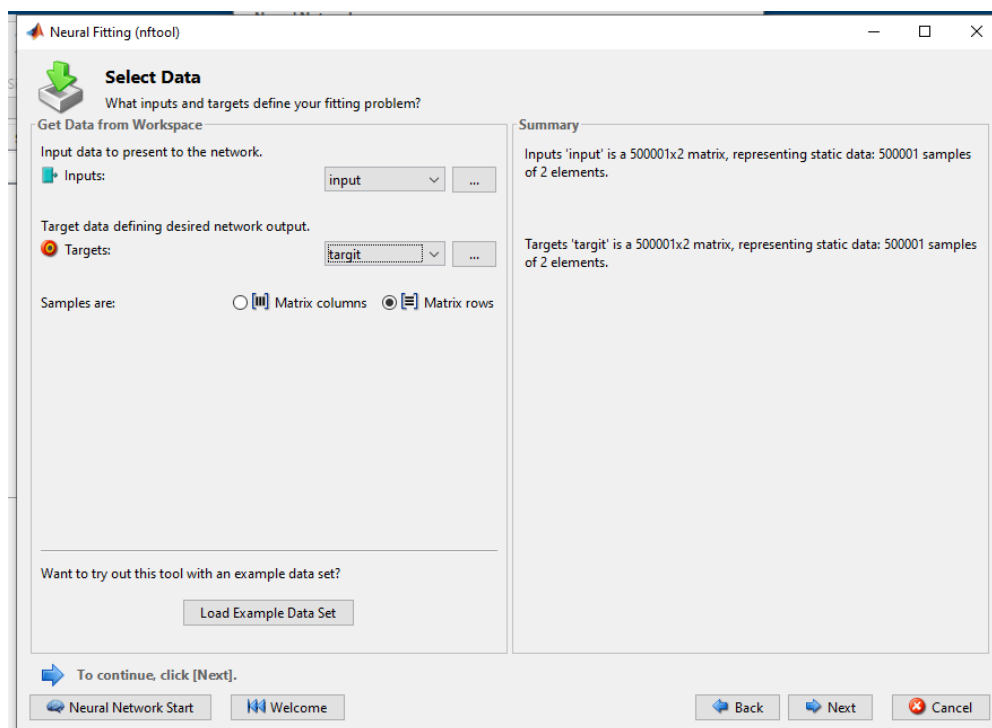


Figure 9. The MATLAB workspace data selection Graphical User Interface (GUI) wizard

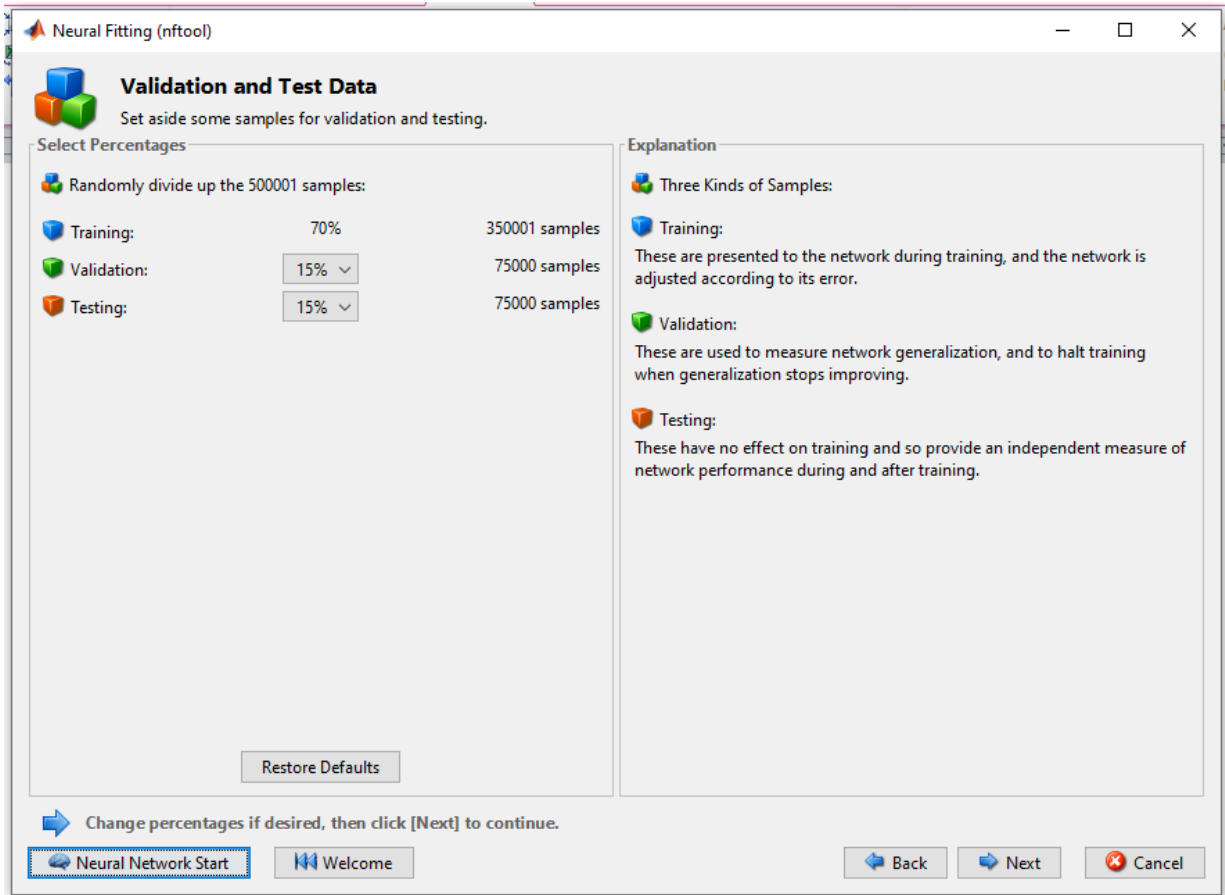


Figure 10. The wizard for testing and validating info

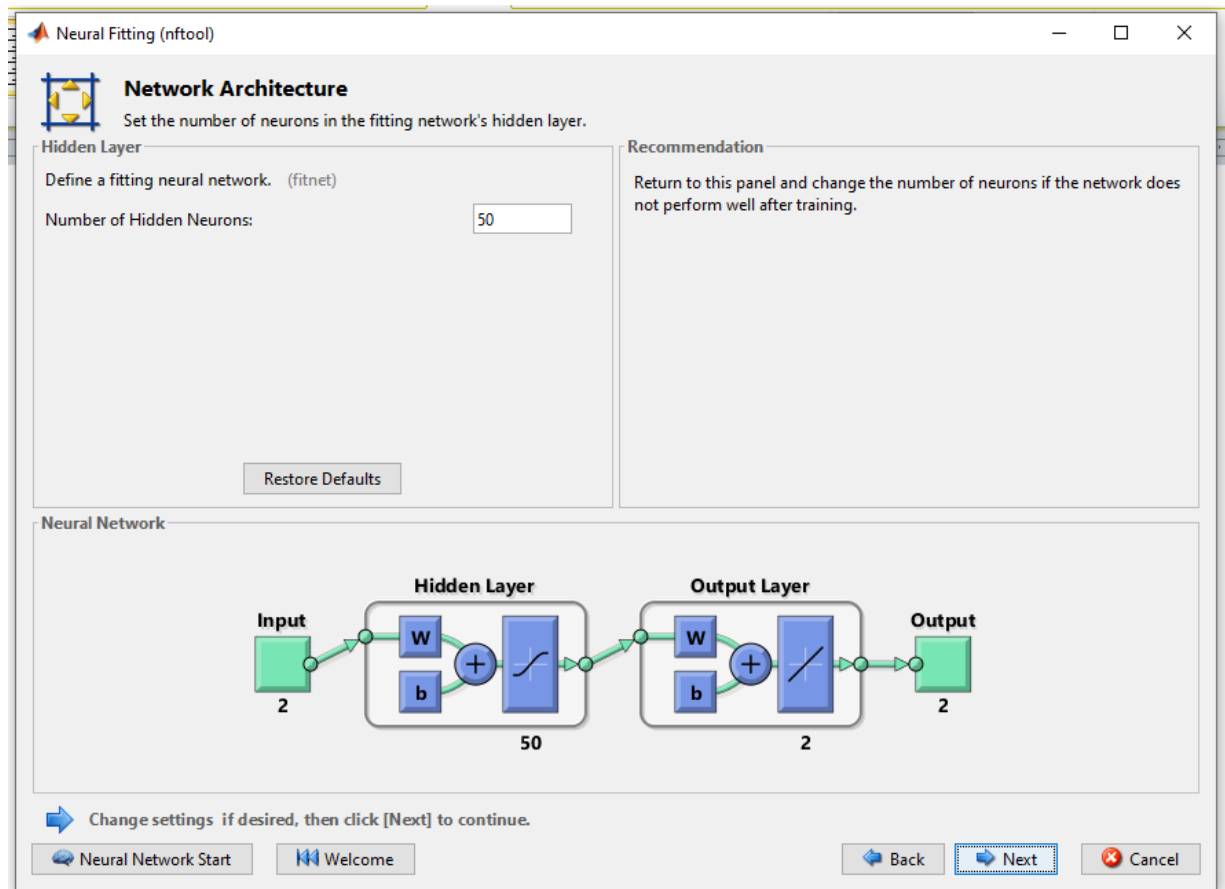


Figure 11. The Artificial Neural Network (ANN) model wizard structure

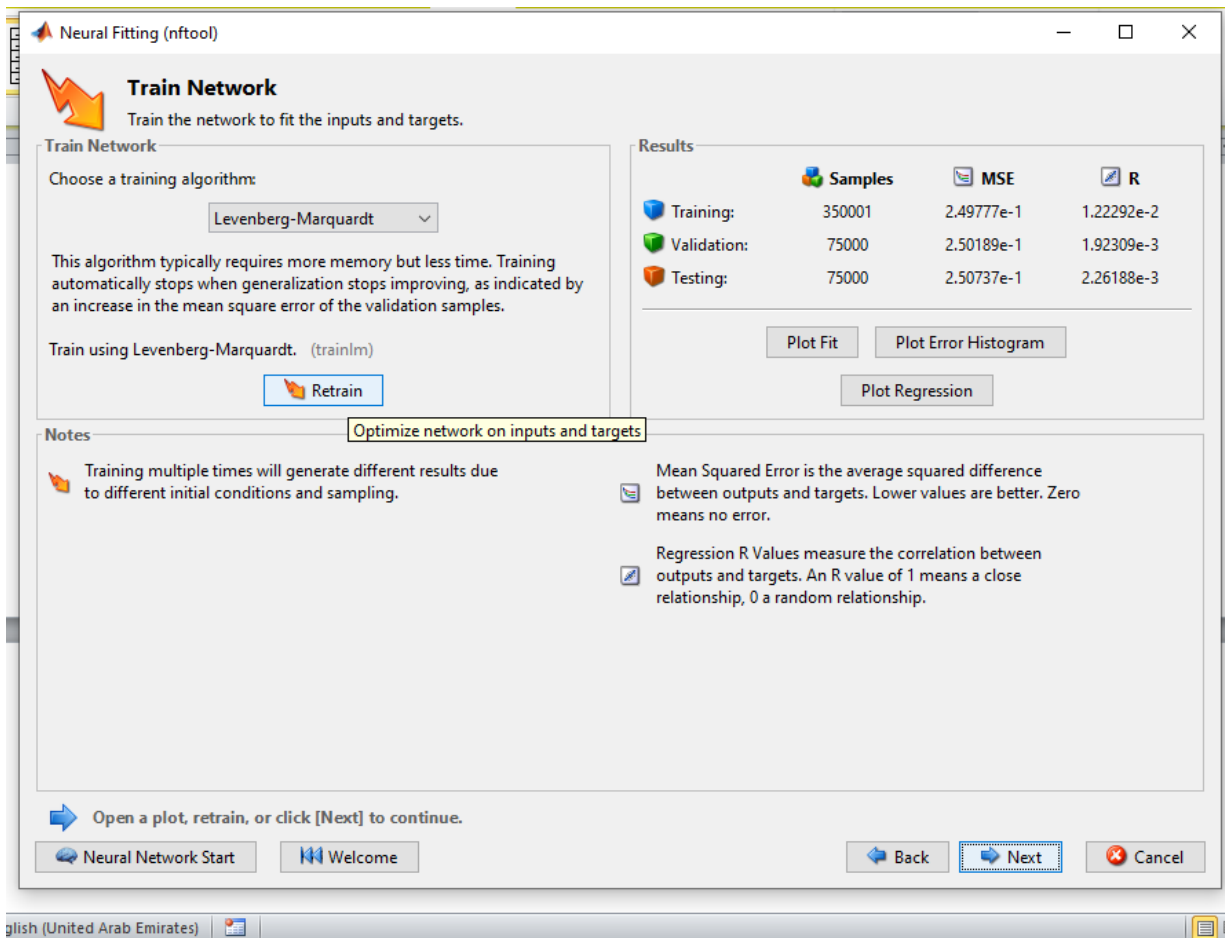


Figure 12. The Artificial Neural Network (ANN) design made use of the railroad network wizard

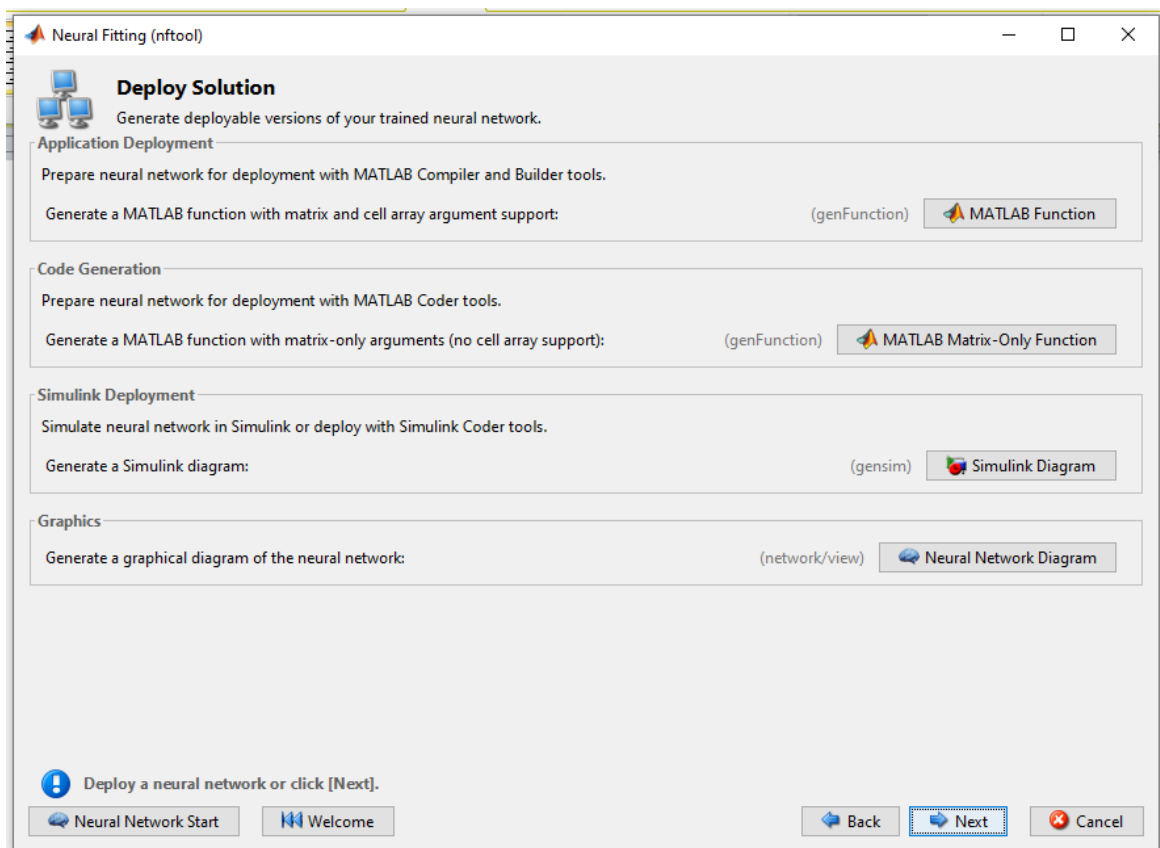


Figure 13. The designed Artificial Neural Network (ANN) deployment solution wizard

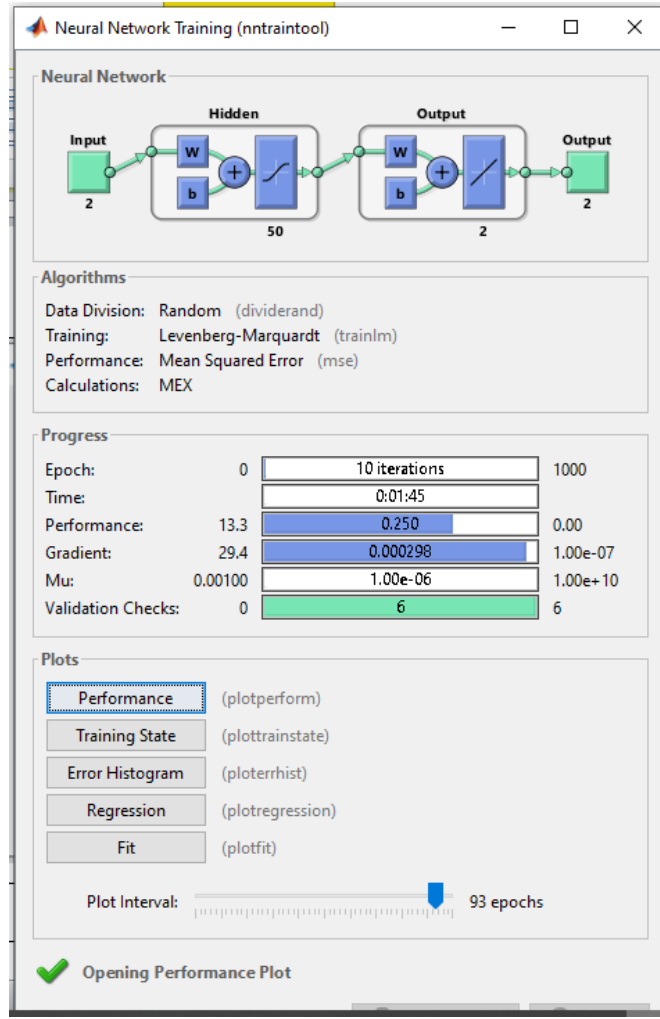


Figure 14. The Artificial Neural Network (ANN) algorithm scheme training designed wizard

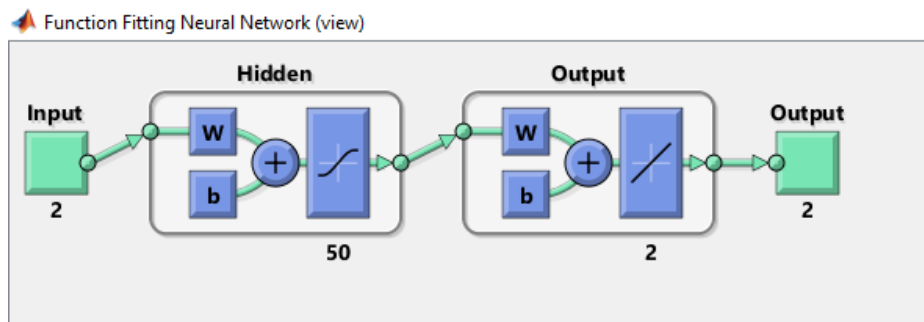


Figure 15. The designed Artificial Neural Network (ANN) algorithm model final structure

As we can see in Figure 13, the design interface application 'nnstart' offers an exceptional and effective platform for creating an ANN algorithm in accordance with the requirements. Neural network diagram options are just a few of the fundamental features this processor offers. These choices will enable the designer to obtain final answers for the ANN model in various formats. For instance, such a wizard may easily create the ultimate Simulink structure of the specified ANN model, which is extremely important to include in the Simulink toolbox against alternative blocks of our proposed model. Figure 14 illustrates the training strategy GUI window for the ANN model that was built.

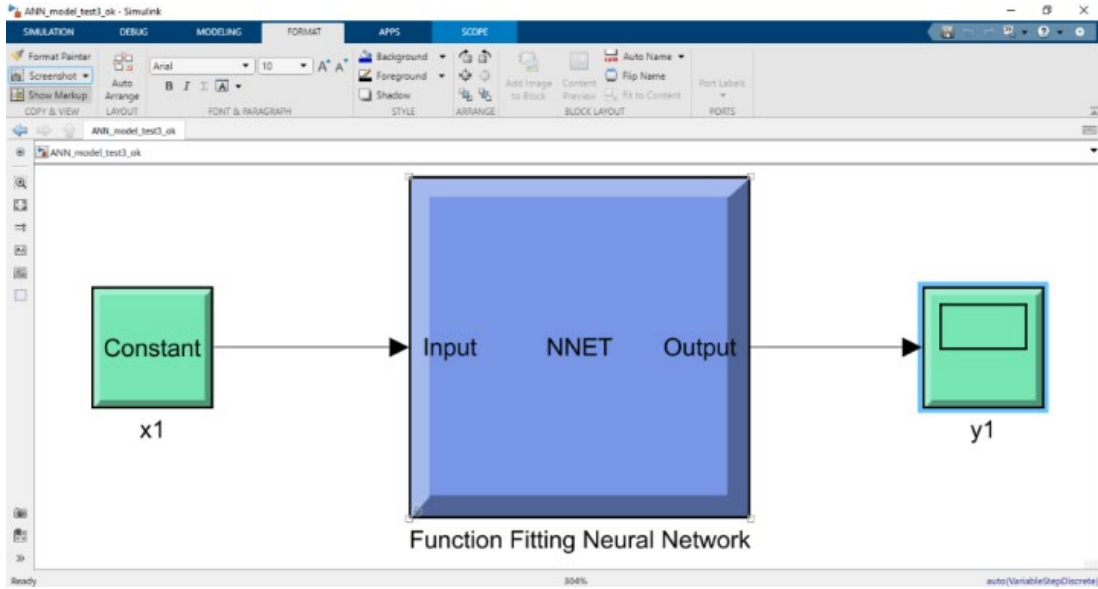
We may infer from looking at Figure 15 that the ultimate construction of the suggested ANN model is designed to consist of 50 hidden layers for the internal neurons learning

weights, along with two input and output layers. Our suggested 5G IoT communication system would use this ANN algorithm model as a deep learning strategy to reduce interference. Figure 16 then presents the completed ANN Simulink structure chart.

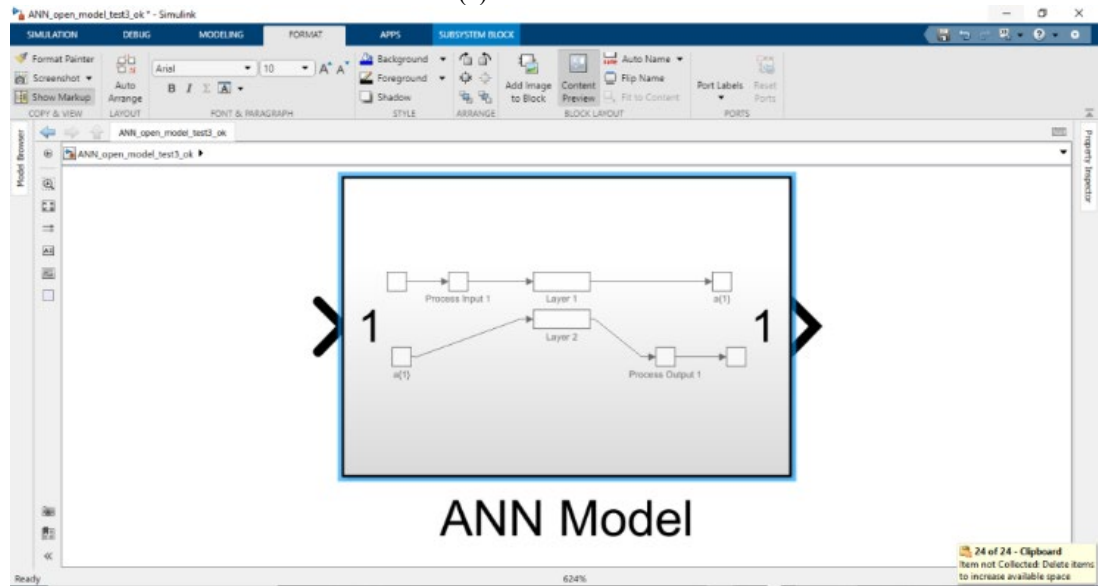
A series of code blocks that represent the inside architecture of the algorithm's operations are included in the simulation of the ANN algorithm, as we can see from the details shown in Figure 16. The three layers that comprise the neural intelligence algorithm, such as the input layer, the hidden layer, and the output layer, as seen in Figure 16 (c) and (d), may then be determined by examining the internal details of the method. Figure 17 also shows the specifics of the developed neurons' internal ANN algorithm hidden layer. As a result, we could witness the numerous planned neurons with

their modified weights that make up the internal hidden layer structure of the ANN algorithm by looking at Figure 17. Additionally, Table 5(a) lists the suggested model design setup

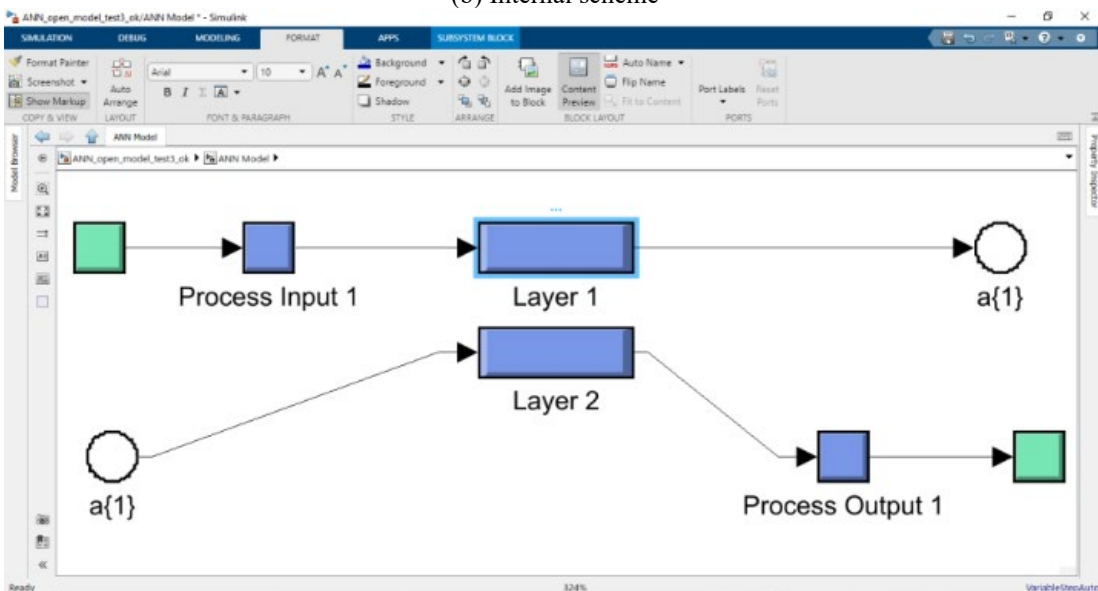
settings for modifying the simulation. Moreover, Table 5(b) illustrates the hyperparameters used in the applied artificial intelligence algorithm.



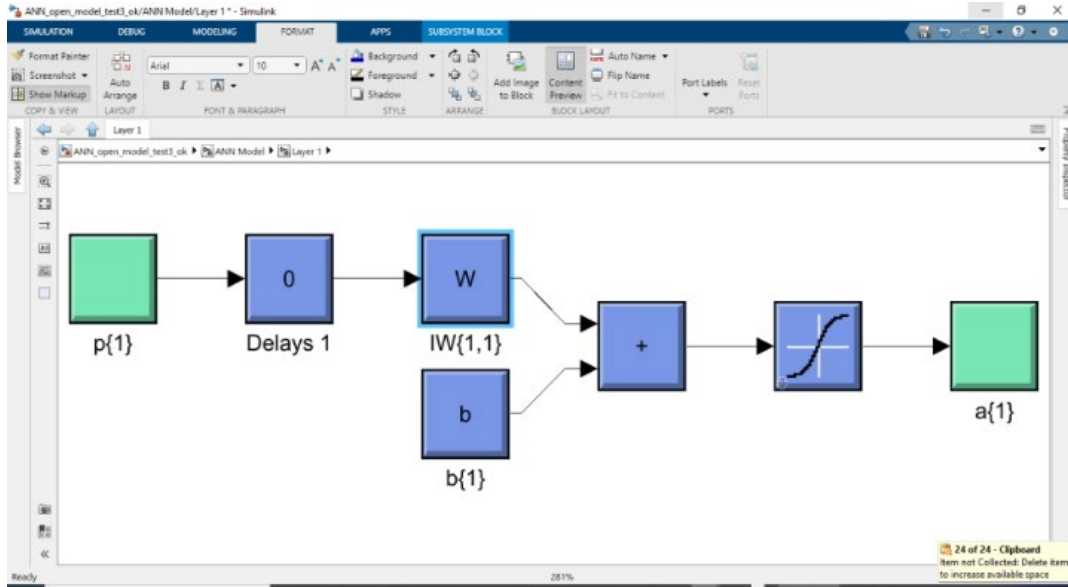
(a) Simulink chart



(b) Internal scheme



(c) Detailed model



(d) Hidden layer structure

Figure 16. The detailed Artificial Neural Network (ANN) Simulink structure view, (a) Simulink structure view, (b) inside view, (c) described model, and (d) creation of the hidden layer

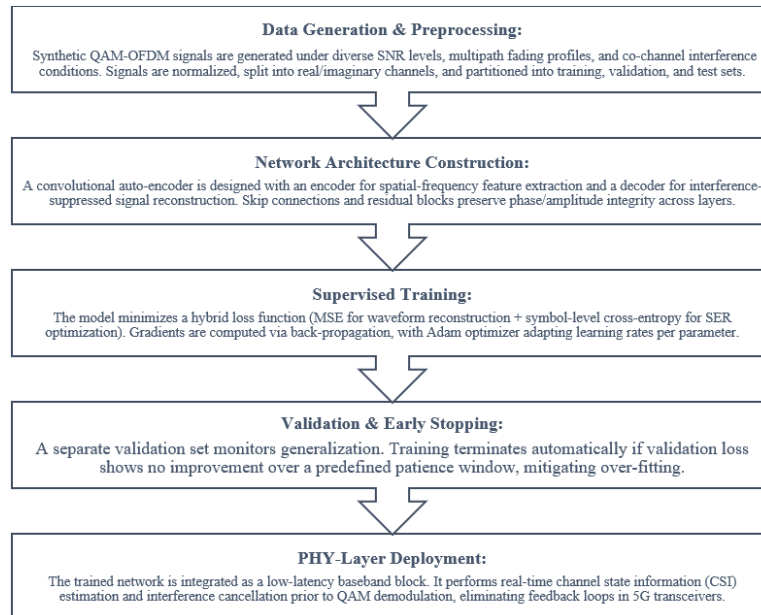


Figure 17. A flowchart showing the steps of the proposed deep learning algorithm

Table 5(a). The necessary design settings and components with specifications used to set the proposed model simulation operation

Model Group	Sampling Frequency (fs)	Transmission Frequency (BW)	Settings Specifics	Construction Group	Remarks
Info Generator 3 Clients	20 MHz	(0-5) MHz	Mean = 0.2 Variance = 0.3 Seed = 1	Random Signal Generator	Employing ADC Rb=3 M bps
Transmitter Model	40 MHz	4 MHz	Bit Rate (Rb) = 2 M bps	OFDM/QPSK	Employing IFFT
Communication Channel	40 MHz	(0-20) MHz	SNR = 5 dB	AWGN With Interference Channel	Bits / symbol = 1
ANN Algorithm	40 MHz	(0-20) MHz	Three layers 10-50 Hidden layers	Employing tanh activation function	Apply Levenberg–Marquardt training
Receiver System	20 MHz	4 MHz	Integration period (number of samples): 8	OFDM/QPSK	Employing FFT

Table 5(b). Demonstration of the hyperparameters used in the applied artificial intelligence algorithm

Hyper-Parameter	Configuration	Rationale / Impact
Learning Rate	1×10^{-4} (step decay: $\times 0.5$ every 20 epochs)	Ensures stable convergence while avoiding local minima in complex-valued loss landscapes
Batch Size	128	Balances GPU memory constraints with accurate gradient estimation
Epochs	150 (Early stopping patience: 15)	Sufficient training cycles with automatic overfitting prevention
Optimizer	Adam ($\beta_1 = 0.9, \beta_2 = 0.999, \epsilon = 1 \times 10^{-8}$)	Adaptive moment estimation for faster convergence under non-stationary channel statistics
Loss Function	Hybrid: MSE + Symbol Cross-Entropy	Jointly minimizes waveform distortion and improves post-demodulation SER/BER
Network Depth	5 Encoder blocks + 5 Decoder blocks	Captures multi-scale channel impairments without excessive computational latency
Kernel Size	3×3 (spatial), 1×7 (frequency)	Extracts localized interference patterns and inter-subcarrier correlations
Activation	LeakyReLU ($\alpha = 0.01$) in hidden layers, Linear in output	Prevents vanishing gradients and preserves complex signal dynamics
Regularization	L2 weight decay ($\lambda = 1 \times 10^{-5}$) + Dropout (rate = 0.2)	Controls model capacity and enhances robustness to unseen channel realizations
Input/Output Format	Complex-valued tensors ($N_{\text{subcarriers}} \times N_{\text{symbols}} \times 2$)	Enables direct I/Q processing compatible with 5G OFDM PHY standards

4. RESULTS AND DISCUSSION

The MatLab2020b Simulink toolbox will be used to simulate and implement the proposed 5G, IoT transceiver network scheme for intervention reduction utilizing deep learning strategy by employing the planned ANN algorithm structure previously described in Section 3. The proposed scheme has been adjusted, and the simulation findings are obtained and presented. The deep learning ANN algorithm's effect has been achieved, and the rebuilt data's final findings are produced and given with thorough explanations.

The data signal flow from the transmitter part via the

channel towards the receiver will be used to show the simulated 5G model's obtained outcomes.

Figure 18 presents the transmitted signal in time and frequency. Figure 19 illustrates the time-domain OFDM waveform and its corresponding spectrum at the output of the digital 5G transmitter. After transmission through the AWGN channel, Figure 20 shows the noisy OFDM signal in both the time and frequency domains. Figure 21 presents the detected analog samples at an SNR of 20 dB before deep learning-based interference cancellation. Finally, Figure 22 shows the samples after the deep learning algorithm.

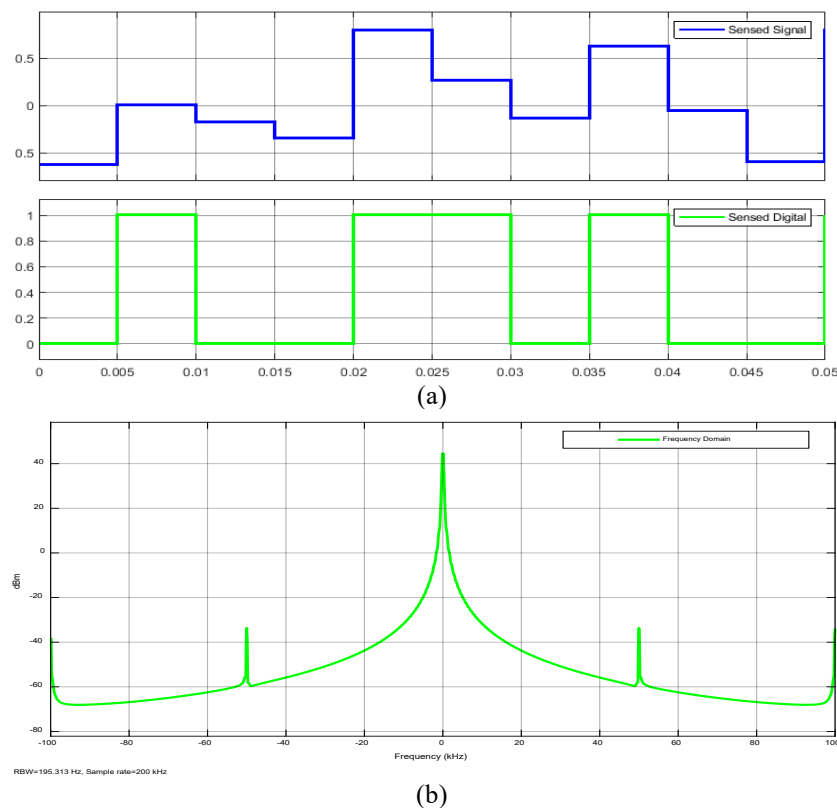
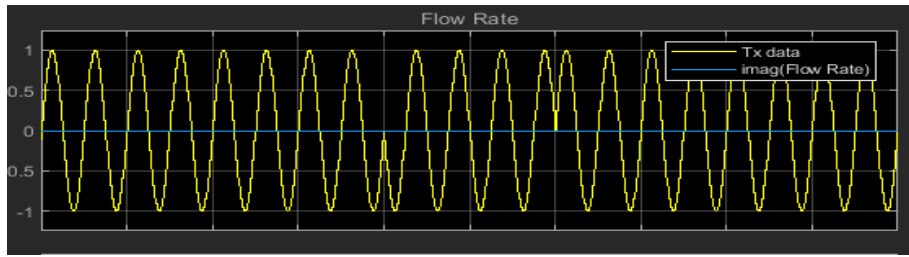
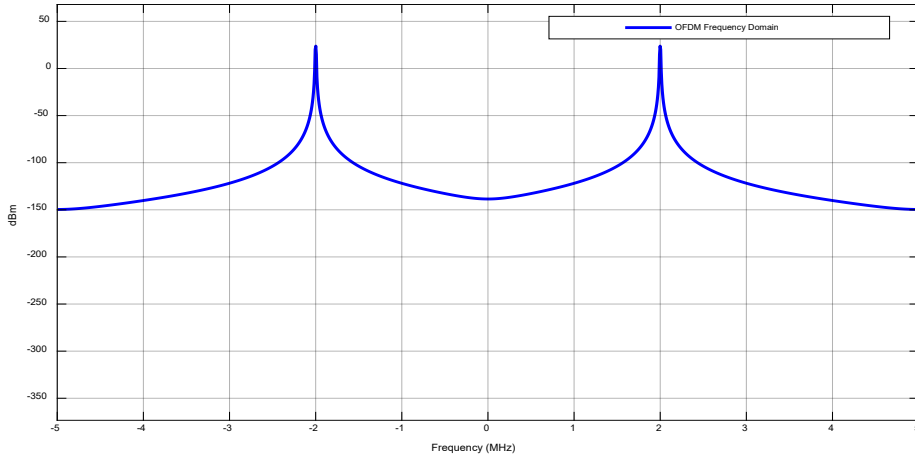


Figure 18. The data signal flow from the transmitter part through the channel towards the receiver is used to show the simulated 5G model's accomplished outcomes, (a) the tested time, (b) frequency spectrum

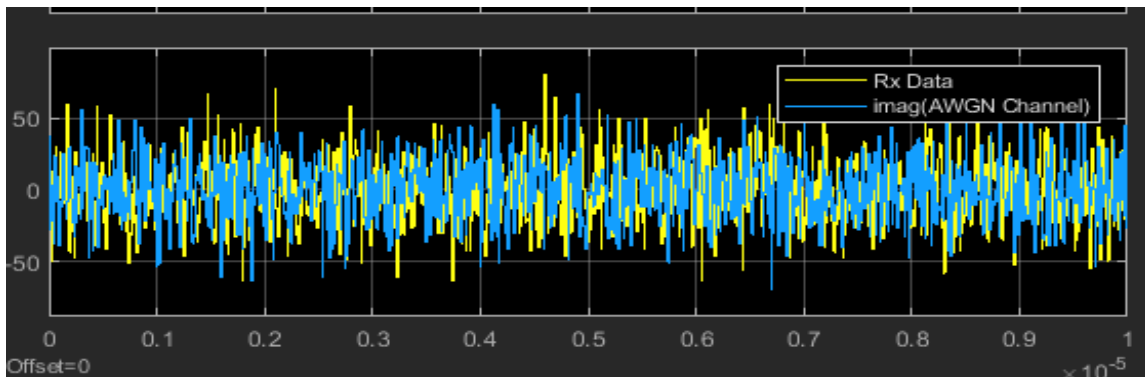


(a)

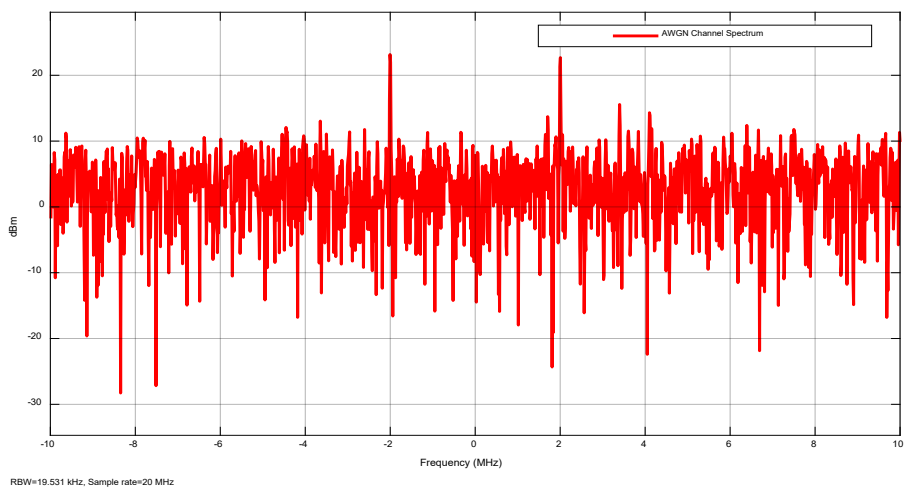


(b)

Figure 19. The spectrum signal at the digital 5G transmitter's output v.s. the orthogonal frequency division multiplexing (OFDM) modulation time, (a) the orthogonal frequency division multiplexing (OFDM) transmitter time signal, (b) frequency waveform at the output of the digital 5G modulator

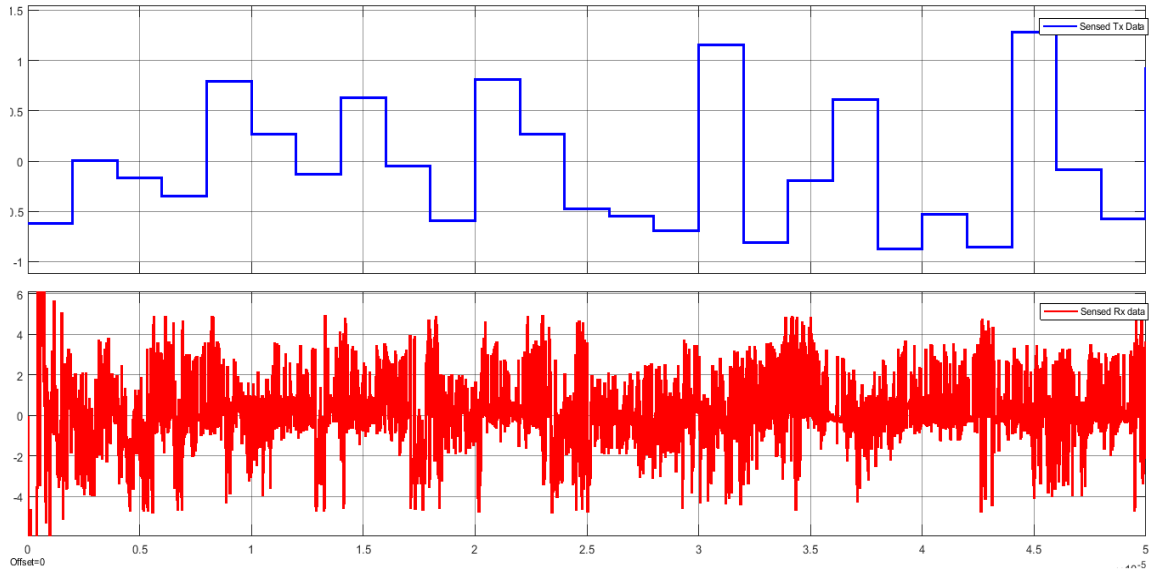


(a)

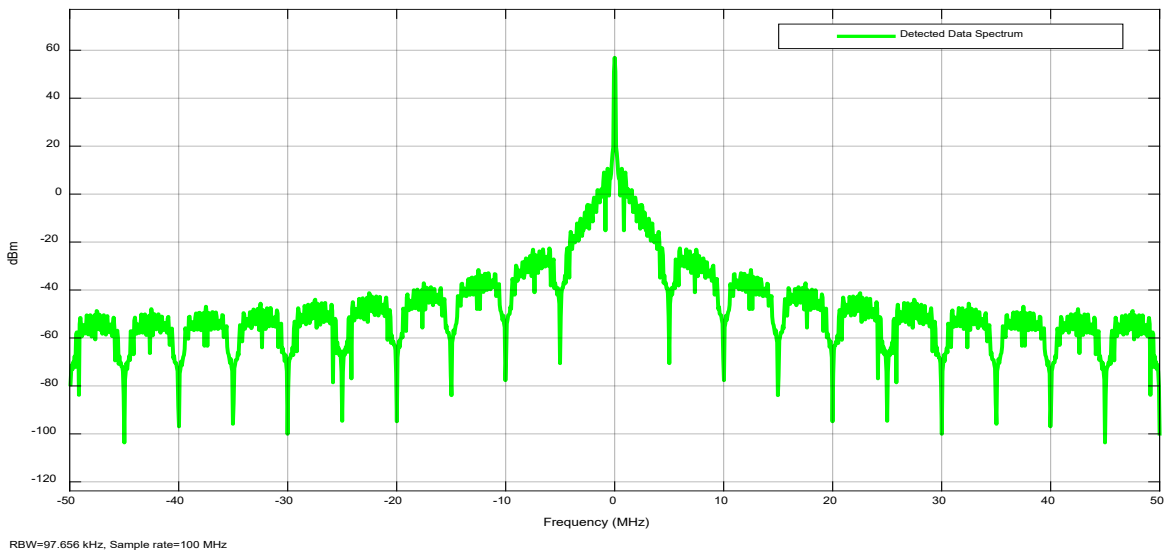


(b)

Figure 20. The spectrum signal at the output of the AWGN noisy transmission medium vs the orthogonal frequency division multiplexing (OFDM) modulation time, (a) AWGN noisy OFDM time signal, (b) The AWGN noisy OFDM spectrum signal

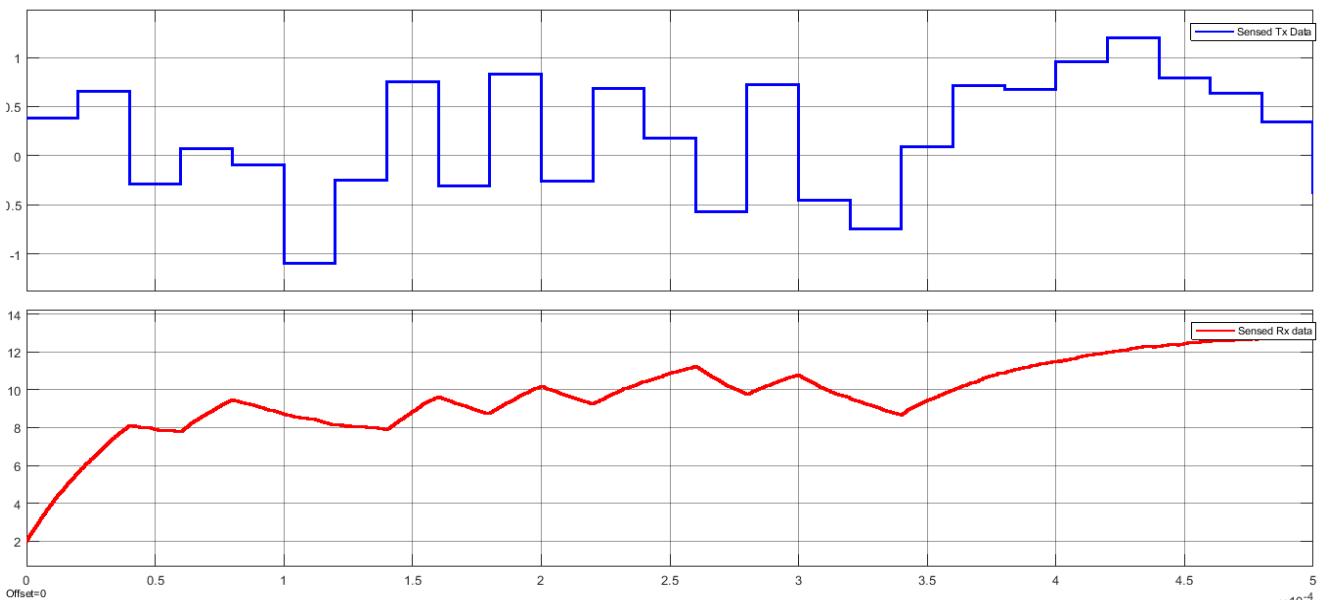


(a)

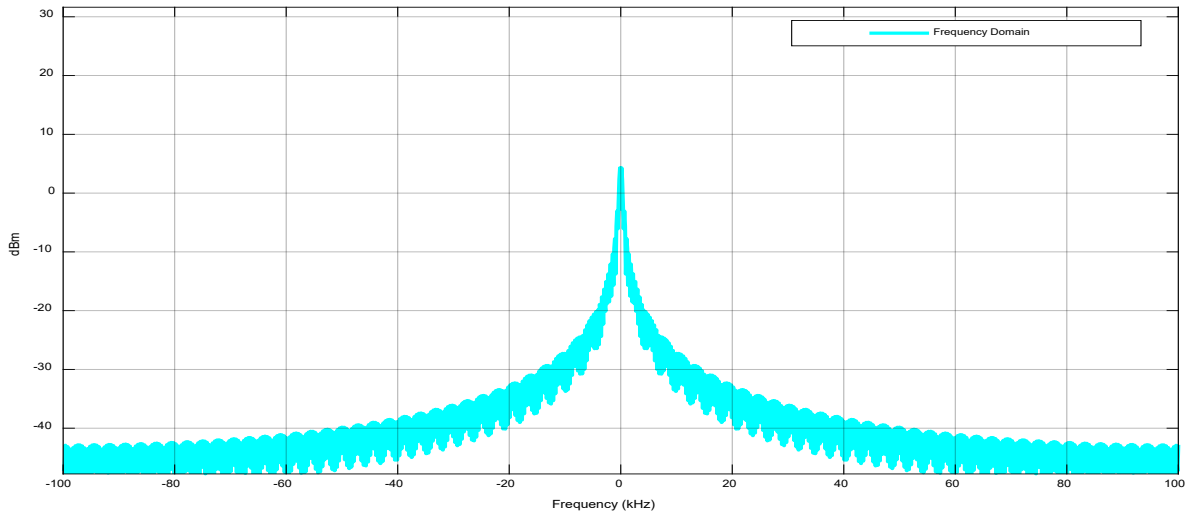


(b)

Figure 21. The time vs. spectrum of the detected analog samples for SNR = 20 dB beyond the impact of the deep learning method, (a) time samples, (b) the frequency spectrum samples



(a)



(b)

Figure 22. The identified analog samples' time vs. spectrum for signal-to-noise ratio (SNR) = 20 dB after the deep learning algorithm's effect, (a) time samples, (b) spectral samples

A) Results Discussions

In order to minimize interference and random noise in the communication channel, deep learning techniques were used to mimic the suggested digital communication model for 5G and IoT technologies. Using the MatLab2020b Simulink tools, the suggested model was put into practice. Based on the findings of this study, a signal processing method that uses a

neural network to address the real-time interference issue in the IoT and 5G wireless communication system was also given. To ascertain the influence of the novel approach on canceling and minimizing the effect of random noise and channel interference signals. Table 6 displays the results of the suggested scheme, which were analyzed with and without the deep learning algorithm impact, as displayed.

Table 6. The final obtained results comparison

Model Group	Signal-to-Noise Ratio (SNR) (dB)	Bit Error Rate (BER)	Error Rate	Efficiency	Resulting Info Quality
Standard Model	10.1	0.98×10^{-1}	24-25%	Weak	High Distortion
Using DL	50.2	0.95×10^{-2}	21-22%	Medium	Medium Distortion
	1.2	0.97×10^{-4}	12%	Very Good	Less Distortion

Table 7. Validation and qualitative comparison of the suggested scheme against recent published articles for the channel estimation 5G mmWave system methods

Performance Metric	Current Study (Hussein and Alhasan)	Tarafder et al. [26]	Ebrahiem et al. [37]	Target/Standard
Symbol Error Rate (SER) @ 20 dB signal-to-noise ratio (SNR)	1.0%	2.5–4.0%	3.1–5.2%	<2.0%
SER Reduction vs. Baseline	15%	8–12%	6–10%	>10%
Bit Error Rate (BER) Improvement	~18%	~10%	~7%	>12%
Throughput Gain	12–18%	5–9%	4–8%	>10%
Inference Latency	10–25 ms	15–40 ms	20–50 ms	<30 ms
Computational Complexity	Medium	High	Medium-High	Low-Medium
Training Data Requirement	Moderate	Large	Large	Minimal
Robustness to Fading	High	Medium	Medium	High
Real-Time Adaptability	Yes	Limited	Limited	Required
Novelty Contribution	"Deep Interference Cancellation" via CNN auto-encoder at physical layer	Systematic classification of pilot contamination & feedback solutions	Methodology for ray-tracing-based dataset generation for DL training	Complementary: Current study adds novel physical-layer DL application

B) Discussion & Validation

The outcomes of the proposed deep learning-based 5G IoT digital communication interference cancellation model have been compared with those examined in contemporary publications and scientific studies. A comprehensive validation of our suggested scheme against that offered by recent published studies is shown in Table 7.

The metrics table uses measurable performance indicators that are directly comparable to earlier efforts to show the quantitative superiority of the suggested paradigm. The recorded data show a notable increase in reaction time, error rates, and bandwidth range, which supports the results' generalizability in dynamic communication settings and strengthens the methodology's trustworthiness.

The foundation for assessing the model's practical viability in 5G contexts is thought to be the analysis of hardware metrics. The results with BER improvement of 18% shown that although minimizing memory and energy usage guarantees the algorithm's compliance with the constrained edge computing resources, short reaction time (10-25%) which minimizes temporal interference. This supports the model's potential deployment on energy-efficient edge processing units with throughput gain of (12-18%), enabling instantaneous estimation independent of the central cloud infrastructure. This integration opens up a wide range of useful applications in industrial IoT and autonomous cars, where local processing speed is crucial to guaranteeing quality of service, by improving the dependability of dense-device networks and lowering the strain on the network backbone.

5. CONCLUSIONS AND RECOMMENDATIONS

In this study, an NN technique integrated with common DSP techniques was proposed to address ISI obstacles in 5G and IoT digital communication technologies. The proposed model was simulated using the Simulink toolkit in MatLab2020b, utilizing an ANN algorithm model to design and implement the proposed 5G and IoT transmission system model to reduce ISI effects. The neural network is integrated to analyze the baseband data rate signal on the physical layer, while ANN are used on the control layer to manage interference in control. By using the proposed ANN model with OFDM-modulated encoded information, the network significantly reduces the symbol error rate (SER). The test and simulation results showed a noticeable improvement in latency, power consumption, memory requirements, and chip area metrics. The user data signal was used in the design model as a representative test data with frequencies up to 20 kHz. The transmission unit was implemented using OFDM technology according to the requirements of 5G communication technologies. Applying the network to the OFDM-modified data leads to a significant reduction in the SER by 15% and an improvement in the BER by 18% compared to conventional methods (such as LMS/RLS filters and LS/MMSE-based estimation). The suggested methodology improved its viability in high-speed applications by boosting bandwidth usage efficiency and attaining a throughput improvement of 12%-18%. Additionally, the system maintained an inference latency between 10 and 25 ms, demonstrating its appropriateness for applications requiring ultra-low latency (Ultra-Reliable Low-Latency Communications) without requiring intricate feedback loops.

Finally, as study recommendations there might be a list of

suggestions for 5G bit rate enhancement using deep learning channel estimation:

1. For quick and precise channel estimate, it is recommended to employ faster CNNs or transformers.
2. Training on Diverse Channels: Boost the model's resilience in practical settings.
3. Implementing Massive MIMO: Multi-channel tracking allows for large data rates.
4. Optimized Models: For low-latency processing, employ quantization and trimming.
5. Making Online Learning Possible: Real-time adaptation to changing surroundings.
6. Improving decoding and lower bit/packet errors by integrating error correction.
7. Employ End-to-End Learning: To maximize efficiency, combine decoding, detection, and estimation.

REFERENCES

- [1] Gallego-Madrid, J., Sanchez-Iborra, R., Ortiz, J., Santa, J. (2023). The role of vehicular applications in the design of future 6G infrastructures. *ICT Express*, 9(4): 556-570. <https://doi.org/10.1016/j.ict.2023.03.011>
- [2] Cai, L., Pan, J., Zhao, L., Shen, X. (2017). Networked electric vehicles for green intelligent transportation. *IEEE Communications Standards Magazine*, 1(2): 77-83. <https://doi.org/10.1109/MCOMSTD.2017.1700022>
- [3] Shah, S.A.A., Ahmed, E., Imran, M., Zeadally, S. (2018). 5G for vehicular communications. *IEEE Communications Magazine*, 56(1): 111-117. <https://doi.org/10.1109/MCOM.2018.1700467>
- [4] Zhang, K., Leng, S., Peng, X., Pan, L., Maharjan, S., Zhang, Y. (2018). Artificial intelligence inspired transmission scheduling in cognitive vehicular communications and networks. *IEEE Internet of Things Journal*, 6(2): 1987-1997. <https://doi.org/10.1109/JIOT.2018.2872013>
- [5] Lee, E.A., Messerschmitt, D.G. (2012). *Digital Communication*. Springer Science & Business Media.
- [6] Agarwal, A., Kumar, B.S., Agarwal, K. (2018). BER performance analysis of image transmission using OFDM technique in different channel conditions using various modulation techniques. In *Computational Intelligence in Data Mining: Proceedings of the International Conference on CIDM 2017*, Springer, Singapore, pp. 1-8. https://doi.org/10.1007/978-981-10-8055-5_1
- [7] Patel, J., Seto, M. (2020). Live RF image transmission using OFDM with RPi and PlutoSDR. In *2020 IEEE Canadian Conference on Electrical and Computer Engineering (CCECE)*, London, ON, Canada, pp. 1-5. <https://doi.org/10.1109/CCECE47787.2020.9255670>
- [8] Rajesh, V., Abdul Rajak, A.R. (2020). Channel estimation for image restoration using OFDM with various digital modulation schemes. *Journal of Physics: Conference Series*, 1706(1): 012076. <https://doi.org/10.1088/1742-6596/1706/1/012076>
- [9] Al-Shably, Z.H., Hussain, Z.M. (2021). Performance of FFT-OFDM versus DWT-OFDM under compressive sensing. *Journal of Physics: Conference Series*, 1804(1): 012087. <https://doi.org/10.1088/1742-6596/1804/1/012087>
- [10] Kansal, L., Gaba, G.S., Chilamkurti, N., Kim, B.G.

- (2021). Efficient and robust image communication techniques for 5G applications in smart cities. *Energies*, 14(13): 3986. <https://doi.org/10.3390/en14133986>
- [11] De Lima, C., Belot, D., Berkvens, R., Bourdoux, A., et al. (2021). Convergent communication, sensing and localization in 6G systems: An overview of technologies, opportunities and challenges. *IEEE Access*, 9: 26902-26925. <https://doi.org/10.1109/ACCESS.2021.3053486>
- [12] Wild, T., Braun, V., Viswanathan, H. (2021). Joint design of communication and sensing for beyond 5G and 6G systems. *IEEE Access*, 9: 30845-30857. <https://doi.org/10.1109/ACCESS.2021.3059488>
- [13] Lees, W.M., Wunderlich, A., Jeavons, P.J., Hale, P.D., Souryal, M.R. (2019). Deep learning classification of 3.5-GHz band spectrograms with applications to spectrum sensing. *IEEE Transactions on Cognitive Communications and Networking*, 5(2): 224-236. <https://doi.org/10.1109/TCCN.2019.2899871>
- [14] Qin, Z., Zhou, X., Zhang, L., Gao, Y., Liang, Y.C., Li, G.Y. (2019). 20 years of evolution from cognitive to intelligent communications. *IEEE Transactions on Cognitive Communications and Networking*, 6(1): 6-20. <https://doi.org/10.1109/TCCN.2019.2949279>
- [15] O'Shea, T.J., Roy, T., Clancy, T.C. (2018). Over-the-air deep learning based radio signal classification. *IEEE Journal of Selected Topics in Signal Processing*, 12(1): 168-179. <https://doi.org/10.1109/JSTSP.2018.2797022>
- [16] Kulin, M., Kazaz, T., Moerman, I., De Poorter, E. (2018). End-to-end learning from spectrum data: A deep learning approach for wireless signal identification in spectrum monitoring applications. *IEEE Access*, 6: 18484-18501. <https://doi.org/10.1109/ACCESS.2018.2818794>
- [17] Xiao, L., Zhang, H., Xiao, Y., Wan, X., Liu, S., Wang, L.C., Poor, H.V. (2019). Reinforcement learning-based downlink interference control for ultra-dense small cells. *IEEE Transactions on Wireless Communications*, 19(1): 423-434. <https://doi.org/10.1109/TWC.2019.2945951>
- [18] Yang, Z., Ding, Z., Fan, P., Karagiannidis, G.K. (2015). On the performance of non-orthogonal multiple access systems with partial channel information. *IEEE Transactions on Communications*, 64(2): 654-667. <https://doi.org/10.1109/TCOMM.2015.2511078>
- [19] Shlezinger, N., Eldar, Y.C., Rodrigues, M.R. (2019). Asymptotic task-based quantization with application to massive MIMO. *IEEE Transactions on Signal Processing*, 67(15): 3995-4012. <https://doi.org/10.1109/TSP.2019.2923149>
- [20] Khani, M., Alizadeh, M., Hoydis, J., Fleming, P. (2020). Adaptive neural signal detection for massive MIMO. *IEEE Transactions on Wireless Communications*, 19(8): 5635-5648. <https://doi.org/10.1109/TWC.2020.2996144>
- [21] Tekbiyik, K., Akbunar, Ö., Ekti, A.R., Görçin, A., Kurt, G.K. (2020). COSINE: Cellular communication signal dataset. *IEEE Dataport*, 20. <http://doi.org/10.21227/safrgh59>
- [22] Rizk, H., Torki, M., Youssef, M. (2019). CellinDeep: Robust and accurate cellular-based indoor localization via deep learning. *IEEE Sensors Journal*, 19(6): 2305-2312. <https://doi.org/10.1109/JSEN.2018.2885958>
- [23] Rizk, H., Abbas, M., Youssef, M. (2021). Device-independent cellular-based indoor location tracking using deep learning. *Pervasive and Mobile Computing*, 75: 101420. <https://doi.org/10.1016/j.pmcj.2021.101420>
- [24] Han, K., Yu, S.M., Kim, S.L., Ko, S.W. (2024). Mobility-induced graph learning for WiFi positioning. *IEEE Journal on Selected Areas in Communications*, 42(7): 1768-1782.
- [25] Tekbiyik, K., Ekti, A.R., Görçin, A., Kurt, G.K., Keçeci, C. (2020). Robust and fast automatic modulation classification with CNN under multipath fading channels. In 2020 IEEE 91st Vehicular Technology Conference (VTC2020-Spring), Antwerp, Belgium, pp. 1-6.
- [26] Dou, F., Lu, J., Xu, T., Huang, T.Y., Xie, J. (2021). A bisection reinforcement learning approach to 3-D indoor localization. *IEEE Internet of Things Journal*, 8(8): 6519-6535. <https://doi.org/10.1109/JIOT.2020.3023711>
- [27] Tekbiyik, K., Akbunar, Ö., Ekti, A.R., Görçin, A., Kurt, G.K. (2019). Multi-dimensional wireless signal identification based on support vector machines. *IEEE Access*, 7: 138890-138903. <https://doi.org/10.1109/ACCESS.2019.2942368>
- [28] Hu, S., Pei, Y., Liang, P.P., Liang, Y.C. (2018). Robust modulation classification under uncertain noise condition using recurrent neural network. In 2018 IEEE global communications conference (GLOBECOM), Abu Dhabi, United Arab Emirates, pp. 1-7. <https://doi.org/10.1109/GLOCOM.2018.8647582>
- [29] Tarafder, P., Chun, C., Ullah, A., Kim, Y., Choi, W. (2025). Channel estimation in 5G-and-beyond wireless communication: A comprehensive survey. *Electronics*, 14(4): 750. <https://doi.org/10.3390/electronics14040750>
- [30] Ebrahimi, K.M., Soliman, H.Y., Abuelenin, S.M., El-Badawy, H.M. (2021). A deep learning approach for channel estimation in 5G wireless communications. In 2021 38th National Radio Science Conference (NRSC) Mansoura, Egypt, 1: 117-125. <https://doi.org/10.1109/NRSC52299.2021.9509813>
- [31] Luan, D., Thompson, J.S. (2023). Channelformer: Attention based neural solution for wireless channel estimation and effective online training. *IEEE Transactions on Wireless Communications*, 22(10): 6562-6577.
- [32] Ye, M., Liang, X., Pan, C., Xu, Y., Jiang, M., Li, C. (2023). Channel estimation for mmWave massive MIMO systems using graph neural networks. In 2023 IEEE/CIC International Conference on Communications in China (ICCC).
- [33] Soltani, M., Pourahmadi, V., Mirzaei, A., Sheikhzadeh, H. (2019). Deep learning-based channel estimation. *IEEE Communications Letters*, 23(4): 652-655. <https://doi.org/10.1109/LCOMM.2019.2898944>
- [34] Le, H.A., Van Chien, T., Nguyen, T.H., Choo, H., Nguyen, V.D. (2021). Machine learning-based 5G-and-beyond channel estimation for MIMO-OFDM communication systems. *Sensors*, 21(14): 4861. <https://doi.org/10.3390/s21144861>
- [35] Zhang, L., Tan, J., Liang, Y.-C., Feng, G., Niyato, D. (2019). Deep reinforcement learning-based modulation and coding scheme selection in cognitive heterogeneous networks. *IEEE Transactions on Wireless Communications*, 18(6): 3281-3294.
- [36] He, H., Wen, C.K., Jin, S., Li, G.Y. (2018). Deep learning-based channel estimation for beamspace mmWave massive MIMO systems. *IEEE Wireless Communications Letters*, 7(5): 852-855. <https://doi.org/10.1109/LWC.2018.2832128>
- [37] Yang, Y., Zhang, S., Gao, F., Ma, J., Dobre, O.A. (2020).

Graph neural network-based channel tracking for massive MIMO networks. IEEE Communications

Letters, 24(8): 1747-1751.